ISSN 0915-633X

NATIONAL INSTITUTE FOR FUSION SCIENCE

Dynamic Structure in Self-Sustained Turbulence

K. Itoh, S.-I. Itoh, M. Yagi and A. Fukuyama

(Received - May 23, 1995)

NIFS-360 June 1995

RESEARCH REPORT
NIFS Series

NAGOYA, JAPAN

Dynamic Structure in Self-Sustained Turbulence

K. Itoh*, S.-I. Itoh†, M Yagi† and A. Fukuyama††

** National Institute for Fusion Science, Nagoya 464-01 Japan*

† Research Institute for Applied Mechanics, Kyushu University 87, Kasuga 816 Japan

†† Faculty of Engineering, Okayama University, Okayama 700 Japan

Abstract

Dynamical equation for the self-sustained and pressure-driven turbulence in toroidal plasmas is derived. The growth rate of the dressed-test mode, which belongs to the subcritical turbulence, is obtained as a function of the turbulent transport coefficient. In the limit of the low fluctuation level, the mode has the feature of the nonlinear instability and shows the explosive growth. The growth rate vanishes when the driven transport reaches to the stationarily-turbulent level . The stationary solution is thermodynamically stable. The characteristic time, by which the stationary and self-sustained turbulence is established, scales with the ion-sound transit time and is accelerated by the bad magnetic curvature. Influences of the pressure gradient as well as the radial electric field inhomogeneity are quantified.

Keywords: Self-sustained turbulence, ballooning mode, interchange mode, anomalous transport, radial electric field gradient, magnetic shear, subcritical turbulence

Contents

1. Introduction

Recently a new theoretical approach to analyze the turbulence and associated anomalous transport in toroidal plasmas has been proposed[1-4]. It has been shown that the nonlinear destabilization mechanism due to the enhanced current diffusivity plays an essential role in determining the turbulence level and transport coefficient. The predicted transport coefficient is in contrast to the conventional argument on the turbulent transport coefficient based on the Kadomtsev formula [5]. The anomalous transport coefficient for the L-mode plasma, which was derived based on the theory of the self-sustained turbulence, explained various aspects of the L-mode plasma confinement, e.g., the dependencies of the energy confinement time τ_E on the plasma current, the internal inductance and the ion mass, as well as the radial profile of the thermal conductivity χ [6]. The analysis has also been done for the intensely heated plasma [7] and has given explanations for the experimental observations on the high-β_p mode [8], PEP mode [9] and current profile control [10]. The theory was extended [11] to include the role of radial electric field [12], in order to quantitatively analyze the confinement of the H-mode [13]. Thermodynamical consideration is made on the turbulence, and the characteristic feature of the non-equilibrium statistical physics was discussed [14]. The comparison with experimental data and the confirmation by the scale invariance method [15] suggest that the theory of the self-sustained turbulence gives promising progress in the understanding of the confinement in a stationary state.

The dynamical change of the transport has been studied theoretically in relation with the L-H transition and the edge localized modes (ELMs) [12,16-19]. The L-H transition has the nature of the bifurcation (first order phase transition) with a hysteresis curve, by which the rapid transition as well as the limit cycle oscillation are possible. The precise analysis of the dynamical evolution would provide a key for the understanding of the turbulence, transport and bifurcation. In the preceding articles, several efforts were done to understand the dynamical evolution. A possible time delay between evolution of the transport coefficient and that of the radial electric field was

modelled in [18] using the quasilinear waves: the quantitative time scales of the L-mode and H-mode confinement are hardly taken into account.

In this article, the study on the temporal evolution of the self-sustained turbulence in toroidal plasmas is made. The fluctuation amplitude and transport coefficients are considered as the dynamical variables. The stability and the temporal evolution near by the stationary solution are first examined. The time rate of the growth/damping of the nonlinear mode, which deviates from the marginally stable condition, is obtained by the perturbation method. Next, the dynamics in the small-amplitude limit is calculated. An explosive growth of the mode is shown when the amplitude is much lower than the stationary level. A formula which smoothly connects these two cases is proposed as well. Influences of the pressure gradient as well as the radial electric field inhomogeneity, as well as the magnetic structure are quantified. The formula serves as a basis for the study of dynamics in the transport phenomena, such as L-H transition and ELMs.

Two cases are investigated, i.e., the case of magnetic hill and that of magnetic well. In the former case, the current-diffusive interchange mode is the relevant mode of the analysis, and the result is applicable to the Heliotron/torsatron configuration. In the latter case, the current-diffusive ballooning mode is subject to the analysis. The obtained formula is applicable to the tokamaks and stellarators. By investigating the interchange mode turbulence in parallel with the ballooning mode turbulence, the generic structure of the dynamics in the plasma turbulence is clarified.

2. Analysis in the Case of the Magnetic Hill

2.1 Model

2.1.1 Model Equation

We study a plasma with magnetic hill in the cylindrical model. The cylindrical coordinate (r,θ,z) is employed. The reduced set of equation [20] is employed. Basic

equations consist of the equation of motion, $n_i m_i\left(\frac{d}{dt}\Delta_\perp\phi - \mu\Delta_\perp^2\phi\right) = B^2\nabla_\parallel J + \frac{B\Omega'}{r}\frac{\partial p}{\partial\theta}$, the Ohm's law, $E + v\times B = J/\sigma - \lambda\Delta_\perp J$ and the energy balance equation $\frac{dp}{dt} = \chi\Delta_\perp p$. In these equations, ϕ is the electrostatic potential, $d/dt = \partial/\partial t + [\phi_0, \ ]$, the bracket [ ] denotes the Poisson bracket, Ω' is the average magnetic curvature, and σ is the conductivity. The transport coefficients μ, λ and χ (ion viscosity, current diffusivity and thermal diffusivity) are obtained by renormalizing the nonlinear interaction with the back ground turbulence, and the explicit derivation is given in [4]. These equations govern the evolution of the dressed-test mode, and the stationary component ϕ_0 is kept in the Poisson bracket.

The eigenmode equation was derived in [21] by use of the Fourier transformation $\tilde{p}(r,\theta,z) = \Sigma \exp(\gamma t + im\theta - inz/R)\int \tilde{p}(k)\exp(-ikx)\,dk$ as

$$\begin{aligned}&\frac{d}{d\hat{k}}\frac{\hat{k}_\perp^2}{\hat{\gamma}+\hat{\lambda}\hat{k}_\perp^4}\frac{d}{d\hat{k}}\left(\hat{\gamma}+\hat{\chi}\hat{k}_\perp^2+\hat{k}_\theta\omega_{E1}\frac{d}{d\hat{k}}\right)p+\frac{G_0}{s^2}p\\&-\frac{1}{\hat{k}_\theta^2 s^2}\left(\hat{\gamma}+\hat{\mu}\hat{k}_\perp^2+\hat{k}_\theta\omega_{E1}\frac{d}{d\hat{k}}\right)\frac{d}{d\hat{k}}\left(\hat{\gamma}+\hat{\chi}\hat{k}_\perp^2+\hat{k}_\theta\omega_{E1}\frac{d}{d\hat{k}}\right)p=0\end{aligned} \qquad (1)$$

In writing Eq.(1), the symbol hat denotes the normalized quantity. We use the normalization $r/a\to\hat{r}$, $t/\tau_{Ap}\to\hat{t}$, $\mu\tau_{Ap}/a^2\to\hat{\mu}$, $\chi\tau_{Ap}/a^2\to\hat{\chi}$, $\lambda\tau_{Ap}/\mu_0 a^4\to\hat{\lambda}$, $\tau_{Ap} = a\sqrt{\mu_0 m_i n_i}/B_p$, $\gamma\tau_{Ap}\to\hat{\gamma}$, γ is the growth rate,

$$G_0 = \Omega'\beta'/2\varepsilon^2 \qquad (2)$$

indicates the magnitude of the energy source for the pressure gradient-driven turbulence, $\varepsilon = r/R$, a and R are the minor and major radii, respectively, and $\beta = 2\mu_0 p/B^2$. The shear parameter s is defined by the relation

$$k_\parallel = kqs(r-r_s)/qR \qquad (3)$$

$q(r_s) = m/n$, and q is the safety factor. Normalized value of $\hat{k}_\theta$ is denoted by the poloidal mode number m, and $\hat{k}_\perp^2 = \hat{k}_\theta^2 + \hat{k}^2$. The parameter ω_{EI} indicates the inhomogeneous radial electric field as

$$\omega_{EI} = \tau_{Ap}\frac{E_r'}{B} \tag{4}$$

The marginal condition which corresponds to the limit $\gamma = 0$, gives the eigen value equation for the stationary turbulent state [21].

2.1.2 Fluctuation Driven Transport

The transport coefficient and the fluctuation amplitude has the relation through the renormalization equation [3] as $\mu = \left(\tilde{\phi}/_{2B}\right)^2 k_\perp^2 \left(\gamma + \mu k_\perp^2\right)^{-1}$ or

$$\mu \cdot \left(\mu + \frac{\gamma}{k_\perp^2}\right) = \left(\frac{\tilde{\phi}}{2B}\right)^2 \tag{5}$$

In this expression, $\tilde{\phi}$ is the average amplitude of the fluctuation potential. The weighting to each Fourier componenets was discussed in [3,4]. The Prandtl numbers of this turbulent state were calculated and were found to remain close to unity [3,4], i.e.,

$$\frac{\hat{\mu}}{\hat{\chi}} \simeq 1 \tag{6}$$

and

$$\frac{\hat{\lambda}}{\hat{\chi}} = \frac{\hat{\mu}_e}{\hat{\chi}}\left(\frac{c}{a\omega_p}\right)^2 \simeq \left(\frac{c}{a\omega_p}\right)^2 \tag{7}$$

where μ_e is the electron viscosity, ω_p is the electron plasma frequency and c is the light velocity.

2.1.3 Nonlinear Growth and Saturation

Equations (4)-(6) represent the relations between μ, χ, λ, γ, and $\tilde{\phi}$. Quantities μ, χ, λ, γ, and $\tilde{\phi}$ are treated as the dynamic variables in this article. In the following subsection, the growth rate γ is expressed in terms on the transport coefficient.

Figure 1 illustrates the growth rate of the dressed test mode as a function of the transport coefficient. When the turbulent-driven transport coefficient is small but finite, the mode growth rate dramatically deviates form that in the linear theory. This regime is called as the 'nonlinear growth' in this article. As the turbulence level further increases, the nonlinear stabilization dominates; the mode growth rate finally vanishes. This state is called as the 'stationary state'.

Figure 1 also shows the schematic drawing of the stability boundary in the plane of the equilibrium pressure gradient and the fluctuation level (Fig.1 (b)). The boundary I denotes the thermodynamically-stable, stationarily-turbulent level. This corresponds to the stationary self-sustained turbulence. The boundary II shows the neutral line for the case of the linearly-stable pressure gradient, i.e., the subcritical turbulence. This is the case for the self-sustained, current-diffusive turbulence. The criterion $|\nabla p_{c,\,lin}|$ indicates the linear stability boundary. Since the boundary II is in the very low amplitude region, we do not discuss the dynamics near the boundary II nor the lienar growth .

Since the transport coefficient, fluctuation amplitude and the growth rate satisfy the relation Eq.(5), the dependence shown in Fig.1 represents the implicit function between the mode growth rate and the fluctuation level. Solving this implicit relation, the nonlinear and explosive growth and saturation of fluctuation amplitude are discussed.

2.2 Dynamics near Stationary State

The temporal evolution in the vicinity of the stationary state is examined. The rate of the dynamic change, γ,near the marginal point is expressed in terms of the

deviation of the dynamical variable (transport coefficient) from the expected value in the stationary state.

2.2.1 Perturbation Method

Equation (1) is expanded with respect to $\hat{\gamma}$, because the growth rate near the stationary condition (γ=0) is analyzed. Keeping the first order correction with respect to $\hat{\gamma}$, we have the equation

$$\hat{\gamma}(L_{t0} + \omega_{E1}L_{t1})\tilde{p} = (L_0 + \omega_{E1}L_1)\tilde{p} \tag{8}$$

where operators L_0, L_1, L_{t0} and L_{t1} are given as

$$L_0\tilde{p} = \frac{\hat{\chi}}{\hat{\lambda}}\frac{d}{d\hat{k}}\frac{1}{\hat{k}_\perp^2}\frac{d}{d\hat{k}}\hat{k}_\perp^2\tilde{p} + \frac{G_0}{s^2}\tilde{p} - \frac{\hat{k}_\perp^6}{\hat{k}_\theta^2 s^2}\hat{\chi}\hat{\mu}\tilde{p} \tag{9}$$

$$L_1\tilde{p} = \frac{\hat{k}_\theta}{\hat{\lambda}}\frac{d}{d\hat{k}}\frac{1}{\hat{k}_\perp^2}\frac{d^2}{d\hat{k}^2}\tilde{p} - \frac{\hat{\chi}}{\hat{k}_\theta s^2}\frac{d}{d\hat{k}}\tilde{p} - \frac{\hat{k}_\perp^4}{\hat{k}_\theta s^2}\hat{\mu}\frac{d}{d\hat{k}}\tilde{p} \tag{10}$$

$$L_{t0}\tilde{p} = -\frac{\hat{\chi}}{\hat{\lambda}^2\hat{k}_\perp^4}\frac{d^2}{d\hat{k}^2}\tilde{p} + \frac{1}{\hat{\lambda}}\frac{d}{d\hat{k}}\frac{1}{\hat{k}_\perp^2}\frac{d}{d\hat{k}}\tilde{p} - \frac{(\hat{\mu}+\hat{\chi})\hat{k}_\perp^4}{\hat{k}_\theta^2 s^2}\tilde{p} \tag{11}$$

$$L_{t1}\tilde{p} = -\frac{\hat{k}_\theta}{\hat{\lambda}^2\hat{k}_\perp^6}\frac{d^3}{d\hat{k}^3}\tilde{p} - \frac{1}{\hat{k}_\theta s^2}\frac{d}{d\hat{k}}\hat{k}_\perp^2\tilde{p} - \frac{\hat{k}_\perp^2}{\hat{k}_\theta s^2}\frac{d}{d\hat{k}}\tilde{p} \tag{12}$$

The operators L_0 and L_{t0} have the even parity, while L_1 and L_{t1} have the odd-parity. The least stable mode in the absence of the radial electric field, i.e., $\omega_{E1} = 0$, has the even-ϕ parity. The radial electric field inhomogeneity, ω_{E1}, mixes the even-ϕ mode and the odd-ϕ mode.

Following the study in the stationary solution [5,21], we use the notation $y = \hat{k} / \hat{k}_0$, $b = \hat{k}_\theta^2 / \hat{k}_0^2$ and $F = b + y^2$ with

$$k_0 = (G_0/\hat{\chi}\hat{\mu})^{1/4} \tag{13}$$

and

$$H = \frac{G_0^{3/2}\hat{\lambda}}{\hat{\chi}^{3/2}\hat{\mu}^{1/2}} \tag{14}$$

We here notice that the eigenvalue H and normalized mode number b are also the dynamical variables, if the turbulence evolves in time. Noting the Prandtl numbers in Eqs.(6) and (7), we see that the normalizing wave number k_0 is in proportion to $\hat{\chi}^{-1/2}$ and that the relation $H \propto \hat{\chi}^{-1}$ holds. The normalization of the wave number to k_0 implies that the characteristic length is stretched according to the turbulence level. The dynamical variable H, which directly correlates with the transport coefficient, is introduced for the transparency of the analysis.

Multiplying $\hat{k}_0^2\hat{\lambda}/\hat{\chi}$ to Eq.(8) and changing the variable from $\hat{k}$ to y, we rewrite Eqs.(9)-(12) to

$$L_0 = \frac{d}{dy}\frac{1}{F}\frac{d}{dy}F + H - \frac{HF^3}{b} \tag{15}$$

$$L_1 = \sqrt{\frac{b}{G_0}}\left\{\sqrt{\frac{\hat{\mu}}{\hat{\chi}}}\frac{d}{dy}\frac{1}{F}\frac{d^2}{dy^2} - \frac{H}{b}\left(\frac{d}{dy}F^2 + \frac{\hat{\mu}}{\hat{\chi}}F^2\frac{d}{dy}\right)\right\} \tag{16}$$

$$L_{t0} = \sqrt{\frac{\hat{\mu}}{\hat{\chi}}}\frac{1}{\sqrt{G_0}}\left(-\frac{d}{dy}\frac{1}{F}\frac{d}{dy} + \frac{G_0}{Hs^2F^2}\frac{d^2}{dy^2} + \frac{(\hat{\chi}+\hat{\mu})}{\hat{\mu}}\frac{HF^2}{b}\right) \tag{17}$$

$$L_{t1} = \sqrt{\frac{b}{G_0}}\left\{Hs^2\sqrt{b}\frac{\hat{\mu}}{\hat{\chi}}\frac{1}{F^3}\frac{d^3}{dy^3} + \frac{H}{G_0\sqrt{b}}\left(\frac{d}{dy}F + F\frac{d}{dy}\right)\right\} \tag{18}$$

Equation (8) is now characterized by the two parameters H and b.

The growth rate $\hat{\gamma}$ as well as the effect of the radial electric field inhomogeneity is calculated by the perturbation method. We write

$$\tilde{p} = u_0 + \rho u_1 \cdots \tag{19}$$

where u_j is the j-th eigen function of the unperturbed equation, $L_0 u_j = 0$. Coefficient ρ indicates the coupling of the even-ϕ mode and odd-ϕ mode due to the inhomogeneous radial electric field. Substituting Eq.(19) into Eq.(8), and operating <1|, we have the relation of ρ as

$$\rho = -\frac{<1|L_1|0> - \hat{\gamma} <1|L_{t1}|0>}{<1|L_0|1> - \hat{\gamma} <1|L_{t0}|1>} \omega_{E1} \tag{20}$$

where the bracket <i|Lj> indicates the integral

$$<i|Lj> = \int_{-\infty}^{\infty} dy u_i(y) L u_j(y) \tag{21}$$

Equation (20) shows the linear relation in between the coupling parameter ρ and ω_{E1}. This reflects the approximation that the radial electric field effect is treated as a perturbation.

From Eqs.(19) and (20), $\tilde{p}$ is expressed in terms of u_0, u_1 and ω_{E1}. Substituting this perturbed expression of $\tilde{p}$ into Eq.(8) and operating <0|, we have

$$\Gamma \hat{\gamma} = <0|L_0|0> - \omega_{E1}^2 \frac{<0|L_1|1><1|L_1|0>}{<1|L_0|1>} \tag{22}$$

where

$$\Gamma = <0|L_0|0> - \omega_{E1}^2 \times \left\{ \frac{<0|L_{t1}|1><1|L_1|0>}{<1|L_0|1>} + \frac{<0|L_1|1><1|L_1|0>}{<1|L_0|1>} \left(\frac{<1|L_{t1}|0>}{<1|L_1|0>} - \frac{<1|L_{t0}|1>}{<1|L_0|1>} \right) \right\} \tag{23}$$

Equation (22) with Eq.(23) describes the growth rate of the dressed-test mode in the vicinity of the stationary solution $\gamma = 0$.

2.2.2 Growth Rate near Steady Sate

For the strongly localized mode, $y^2 < 1$, the eigen value equation $L_0 p = 0$ was approximated as the Weber type equation. The zero-th and first eigen functions are given as $u_0 = \xi^{1/4}\pi^{-1/2}\exp(-\xi y^2/2)$ and $u_1 = \sqrt{2/\pi}\xi^{3/4} y \exp(-\xi y^2/2)$. By the help of this approximation, the analytic evaluation of the integrals in Eqs.(22) and 923) becomes possible.

At the stationary condition, which is indicated in Fig.1, the dynamical variable H takes the eigen value H_0. (The suffix 0 denotes the stationary state, $\hat{\gamma} = 0$.) For the least stable mode, the eigenvalue H_0 was calculated as [4]

$$H_0 = 1.26 \tag{24}$$

and $\xi^2 = 3bH_0$ for the mode number of

$$b = 0.34. \tag{25}$$

The growth rate does not vanish if the dynamical variable H is not equal to H_0. The right hand side of Eq.(22) was calculated in [21] and was given as

$$<0|L_0|0> - \omega_{E1}^2 \frac{<0|L_1|1><1|L_1|0>}{<1|L_0|1>} = \xi(1 + h_1\omega_{E1}^2)\left(\frac{\hat{\chi}_{H0}}{\hat{\chi}} - 1\right) \tag{26}$$

The term $\hat{\chi}_{H0}$ represents the statistical expected value of the thermal diffusivity in the presence of the radial electric field inhomogeneity. In other words, the dynamical variable $\hat{\chi}$ is predicted to take the value $\hat{\chi}_{H0}$ in the stationary state. (Since the thermal conductivity which would be relevant to the H-mode plasma is that for the case in the presence of the electric field. We therefore abbreviate it as the transport coefficient in the 'H-mode plasma'.) The transport coefficient $\hat{\chi}_{H0}$ is given as

$$\hat{\chi}_{H0} \equiv \frac{\hat{\chi}_{L0}}{(1 + h_1\omega_{E1}^2)} \tag{27}$$

with

$$h_1 \simeq \frac{0.52}{G_0} \tag{28}$$

and

$$\hat{\chi}_{L0} \equiv \frac{G_0^{3/2}}{H_0 s^2} \frac{\hat{\lambda}}{\hat{\chi}} \sqrt{\frac{\hat{\chi}}{\hat{\mu}}} \simeq \frac{G_0^{3/2}}{H_0 s^2} \frac{c^2}{a^2 \omega_p^2} \tag{29}$$

$\hat{\chi}_{L0}$ is the transport coefficient for the stationary state in the absence of the radial electric field inhomogeneity i.e., that in the stationary L-mode plasma.

The same eigen functions are used to evaluate the integrals in the coefficient Γ in Eq.(23). Explicit form of integrals <i|Lj> are given in the appendix A. Taking the lowest order terms with respect to G_0, we have

$$\Gamma \simeq \frac{H\left(2b + \frac{3}{2\xi}\right)}{G_0^{1/2}} \left[1 + \frac{2\xi}{4b\xi + 3} \frac{\omega_{E1}^2}{G_0} \times \left\{ \frac{b^{3/2} C_2}{\xi^{1/2}} - \frac{2b^2 C_1 C_2}{\xi^2} \left(b + \frac{9}{4\xi} - \frac{\xi^{3/2}}{\sqrt{2b} C_2} \right) \right\} \right] \tag{30}$$

with $C_1 = \{3b\xi/4 - 3/8 + H_0(b^2 + b/\xi + 3/4\xi^2)\}$ and $C_2 = C_1 - 1/2$. In obtaining Eq.(30) we use the simplification $F \approx b$. Substituting the absolute values of $H_0 = 1.26$, $b = 0.34$ and $\xi = 1.03$ into Eq.(30), we have $\Gamma = \frac{2H}{\sqrt{G_0}} \left(1 + \frac{0.02}{G_0} \omega_{E1}^2 \right)$. Substituting this expression of Γ into Eq.(22) and using Eq.(26), Eq. (22) is written as

$$\frac{2H}{\sqrt{G_0}} \left(1 + \frac{0.02}{G_0} \omega_{E1}^2 \right) \hat{\gamma} = \xi \left(1 + h_1 \omega_{E1}^2 \right) \left(\frac{\hat{\chi}_{H0}}{\hat{\chi}} - 1 \right) \tag{31}$$

We notice the relations $H/H_0 = \hat{\chi}_{L0}/\hat{\chi}$ and Eq.(27), and the variable H in the left hand side of Eq.(31) is expressed in terms of the dynamical variable $\hat{\chi}$ as $H = H_0 \hat{\chi}_{H0} (1 + h_1 \omega_{E1}^2) / \hat{\chi}$. Using this identity, Eq.(31) is rewritten as

$$\hat{\gamma} = \frac{\xi}{2H_0} \frac{\sqrt{G_0}}{\left(1 + \frac{0.02}{G_0}\omega_{E1}^2\right)} \frac{\hat{\chi}}{\hat{\chi}_{H0}} \left(\frac{\hat{\chi}_{H0}}{\hat{\chi}} - 1\right) \tag{32}$$

Using the estimation $\xi/2H_0 = 0.45$, we finally have the explicit formula of the growth rate as

$$\hat{\gamma} = \frac{0.45\sqrt{G_0}}{\left(1 + \frac{0.02}{G_0}\omega_{E1}^2\right)} \left(1 - \frac{\hat{\chi}}{\hat{\chi}_{H0}}\right) \tag{33}$$

This result shows that the fluctuation amplitude grows in time, in the case of

$$\hat{\chi} < \hat{\chi}_{H0} \qquad \text{or} \qquad \frac{T}{eB}\frac{e\tilde{\phi}}{T} < \chi_{H0} \tag{34}$$

On the contrary, the mode amplitude damps if $\hat{\chi}$ exceeds $\hat{\chi}_{H0}$ ($\tilde{\phi}/B > \chi_{H0}$). The stationary solution of a strongly-turbulent state

$$\hat{\chi} = \hat{\chi}_{H0} \qquad \text{or} \qquad \left(\frac{T}{eB}\frac{e\tilde{\phi}}{T} = \chi_{H0}\right) \tag{35}$$

is thermodynamically stable.

2.3 Nonlinear Growth in Low Fluctuation Limit

The dressed test mode has nonlinear growth rate in the limit of small fluctuation amplitude as is shown in Fig.1. The analytic formula for the nonlinear growth rate is derived in the small but finite amplitude limit. Then a connection formula of the growth rate between the small amplitude state and that near the large-amplitude stationary state is discussed.

2.3.1 Nonlinear Growth Rate

The growth rate in the limit of the small fluctuation amplitude (i.e., small transport coefficient), $\hat{\chi}\hat{k}_\perp^2 < \hat{\gamma}$, was discussed in [3]. It was found that the growth rate has the dependence like $\hat{\gamma} \propto \hat{\lambda}^{1/5}$ in the small $\hat{\lambda}$ limit. The formula is extended here to the case where the electric field gradient is present. Derivation is given in the appendix B, and the growth rate is given as

$$\hat{\gamma} = \frac{\hat{\gamma}_0}{1 + \frac{9}{20}\frac{\omega_{E1}^2}{G_0}} \tag{36-1}$$

and

$$\hat{\gamma}_0 = 2^{4/5} 3^{-3/5} G_0^{3/5} \hat{\lambda}^{1/5} s^{-2/5} \hat{k}_\theta^{4/5} \tag{36-2}$$

This result confirms that the growth rate has the dependence on the transport coefficient as $\hat{\gamma} \propto \hat{\lambda}^{1/5}$ and indicates that the nonlinear growth rate is reduced by the electric field inhomogeneity. It should be also noted that the shorter wave length mode has larger growth rate. This dependence on k_θ continues so long as the effect of thermal diffusion is weak, i.e., $\hat{\gamma} > \hat{\chi}\hat{k}_\perp^2$. If k_θ becomes too large, the stabilization by thermal diffusion and viscosity dominates, and the mode becomes stable. Using the estimate $k_\perp \sim k_\theta$ and Eq.(36), the relation $\hat{\gamma} > \hat{\chi}\hat{k}_\perp^2$ is approximately written as

$$k_\theta < \left(\frac{\hat{\chi}}{\hat{\lambda}}\right)^{1/2} s\, G_0^{-1/2} \left(\frac{\hat{\chi}_{H0}}{\hat{\chi}}\right)^{4/5} \tag{37}$$

Figure 2 illustrates the unstable region of the dressed test mode in the k_θ-χ plane. The least stable mode determines the stationary level of the transport coefficient. The peak of the growth rate moves towards the shorter wave length mode if the diffusivities becomes smaller than those in the stationary value. The normalization of the mode number, Eq.(13), implies that the mode number which gives the peak of the growth rate may depend like $k_\theta \propto \hat{\chi}^{-1/2}$, as $\hat{\chi}/\hat{\chi}_{H0}$ becomes smaller.

The growth rate Eq.(36) is evaluated for the mode number $\hat{k}^*$, which is characteristic to the steady state turbulence. Near the stationary state, $\tilde{\phi} / B \approx \chi_{H0}$, the characteristic mode number for the turbulence, $\hat{k}^*$, is estimated. Using the eigenvalue of b for the stationary state, $b \approx 0.34$, the normalization $\hat{k}_\theta = \sqrt{b} k_0$ gives the relation of k_θ and the transport coefficient as $\hat{k}_\theta = 0.58(G_0/\hat{\chi}\hat{\mu})^{1/4}$. Substituting the values in the stationary state, $\hat{\chi}_{H0}$ and $\hat{\mu}_{H0}$, in this expression, we have the estimate

$$\hat{k}^* = 0.58(G_0\hat{\chi}/\hat{\mu})^{1/4}\hat{\chi}_{H0}^{-1/2} \tag{38}$$

If one fixes the mode number as $\hat{k}_\theta = \hat{k}^*$, and substitutes this form of k_θ, the relation $(\hat{\chi}/\hat{\mu})^{1/5} \simeq 1$ and the expression of $\hat{\chi}_{H0}$ (i.e., Eq.(27)) into Eq.(36), we have

$$\hat{\gamma} = \frac{0.58\, G_0^{1/2}}{1 + \left(\frac{9}{20} - \frac{h_1}{5}\right)\frac{\omega_{E1}^2}{G_0}}\left(\frac{\hat{\chi}}{\hat{\chi}_{H0}}\right)^{1/5} \approx \frac{0.58\, G_0^{1/2}}{1 + 0.35\frac{\omega_{E1}^2}{G_0}}\left(\frac{\hat{\chi}}{\hat{\chi}_{H0}}\right)^{1/5} \tag{39}$$

in the limit of $\hat{\chi} << \hat{\chi}_{H0}$. In deriving this result we employ the approximation $(1 + h_1\omega_{E1}^2)^{1/5} \simeq 1 + \frac{h_1}{5}\omega_{E1}^2$.

2.3.2 Connection Formula

Comparing Eqs.(33) and (39), we see that $\hat{\gamma}$ scales as $\sqrt{G_0}$ both in the small amplitude limit and near the stationary state. In the small $\hat{\chi}$ limit, it has a dependence as $(\hat{\chi} / \hat{\chi}_{H0})^{1/5}$; near the stationary state, it behaves like $\hat{\gamma} \propto (1 - \hat{\chi} / \hat{\chi}_{H0})$. Combining Eqs.(33) and (39), a connection formula of the growth rate for the mode with $\hat{k}_\theta = \hat{k}^*$ is given as

$$\hat{\gamma} \simeq \frac{0.5\, G_0^{1/2}}{1 + \frac{0.35\omega_{E1}^2}{G_0}}\left(\frac{\hat{\chi}}{\hat{\chi}_{H0}}\right)^{1/5}\left(1 - \frac{\hat{\chi}}{\hat{\chi}_{H0}}\right) \tag{40}$$

As is illustrated in Fig.2, the modes with larger mode numbers, $k_\theta > k^*$, become more unstable in the case of the lower fluctuation level, $\hat{\chi} << \hat{\chi}_{H0}$. The wave number of the mode, which is most unstable for the given value of $\hat{\chi}$, increases as $\hat{\chi}$ is reduced from $\hat{\chi}_{H0}$. Figure 3 illustrates the schematic growth rate as a function of the thermal diffusivity χ. One would draw an envelope of the peaks of the growth rate for various modes. The largest growth rate in the small χ limit with $\omega_{E1} = 0$ was given as

$$\hat{\gamma} \simeq 0.5 G_0^{1/2} \tag{41}$$

which corresponds to the growth rate of the fast interchange mode [22]. From Eqs.(33) and (41), we see that the formula Eq.(33) is an approximation for the envelope of the least stable modes. Equation (33) can be used as a connection formula for the growth rate of the turbulent fluctuations in the system of the magnetic hill.

Two distinct features are seen in the formula (33). (i) The growth rate is described by the geometrical parameters and the pressure gradient. It does not include the dissipation coefficient. (ii) There is no critical pressure gradient for this fast rate of the change. These results show a clear contrast to the conventional argument based on the quasi-linear formalism [5]. The first aspect, i.e., γ is independent of the dissipation rate (such as resistivity) as is in the ideal MHD theory, indicates that the change of turbulence can occur in a rapid time scale. When the turbulent level and associated transport coefficient are deviated from the values of the stationary state, the characteristic time scales for the growth (if $\chi < \chi_{H0}$) and damping (if $\chi > \chi_{H0}$) is of the order of $\tau_{Ap} G_0^{-1/2}$, i.e., the combination of the ion sound transit and the bad magnetic curvature. The scaling with the ion-sound transit time suggests that the very rapid change of fluctuation level is predicted. This time scale is of the order of the linear ideal MHD modes [22]. The second aspect of γ, i.e., $\hat{\gamma} \propto G_0^{1/2}$, indicates that this rapid change occurs at any pressure gradient (i.e., independnet of the linear ideal MHD instability condition), if the state deviates from the marginal point, $\hat{\chi} = \hat{\chi}_{H0}$.

2.4 Explosive Growth and Saturation

The plasma turbulence has the nature of the sub-critical turbulence [1-4], and the nonlinear growth rate dominates the linear growth rate at the very low level of the fluctuation amplitude. Numerical simulation has been done and the strong nonlinear instability has been found [23]. The relation between the growth rate and the dynamical variables are given as Eqs.(33) or (40). Using these relations, we study the temporal evolution of the fluctuation amplitude.

2.4.1 Explosive Growth

First, the dynamics in the small amplitude limit is analytically studied. Equation (5) provides the relation $\chi \cdot \left(\chi + \gamma k_\perp^{-2}\right) = \left(\tilde{\phi} / 2B\right)^2$ with the help of the assumption $\chi \simeq \mu$. In the regime of the nonlinear growth, $\hat{\gamma} \propto \hat{\lambda}^{1/5}$, the term $\chi\,\gamma k_\perp^{-2}$ is of the lower power in terms of χ than the term χ^2. (In other words, the decorrelation time in the propagator is given by γ rather than $\chi k_\perp^2$.) In this case we have

$$\chi \cdot \gamma k_\perp^{-2} \simeq \left(\tilde{\phi} / 2B\right)^2. \tag{42}$$

Substituting Eq.(39) into Eq.(42) and using Eqs.(27)-(29), we have the expression of χ in terms of ϕ as

$$\frac{\hat{\chi}}{\hat{\chi}_H} \approx \frac{1.57}{\left(1 + 0.14\, G_0^{-1}\omega_{E1}^2\right)} \frac{G_0^{5/6}}{s^{5/3}} \left(\frac{c}{a\omega_p}\hat{k}_\perp\right)^{5/3} \hat{\phi}^{5/3} \tag{43}$$

where $\hat{\phi}$ is the absolute value of the amplitude that is normalized as

$$\hat{\phi} = \frac{\tilde{\phi}}{2B} \frac{1}{\chi_{H0}} \tag{44}$$

The mode amplitude is normalized such that $\hat{\phi} = 1$ at the saturation level. In deriving Eq.(43), we employ the simplification $\hat{\mu} / \hat{\chi} \simeq 1$ and $\hat{\lambda} / \hat{\chi} \simeq \left(c / a\omega_p\right)^2$. It is noted that

the thermal diffusivity scales like $\chi \propto \phi^{5/3}$. This dependence is in between that of the quasilinear approximation, $\chi \propto \phi^2$, and the one for the strong turbulence, $\chi \propto \phi$. The power index of 5/3 is characteristic to the strong nonlinear growth phase.

The growth rate is now expressed in terms of $\hat{\phi}$. By substituting Eq.(43) into Eq.(39), as

$$\hat{\gamma} \approx \hat{\gamma}_n \hat{\phi}^{1/3} \tag{45}$$

where

$$\hat{\gamma}_n \approx \frac{0.61}{1 + 0.38\frac{\omega_{E1}^2}{G_0}} G_0^{2/3} s^{-1/3} \left(\frac{c}{a\omega_p}\hat{k}_\perp\right)^{1/3} \tag{46}$$

is expressed in terms of the equilibrium parameter and the mode number. The dynamical equation, which describes the evolution of the mode amplitude, is reduced from Eq.(45) as

$$\frac{d}{d\hat{t}}\hat{\phi} = \hat{\gamma}_n \hat{\phi}^{4/3} \tag{47}$$

for small but finite amplitude, $\hat{\phi} << 1$. This equation is solved analytically, and the solution is written explicitly as

$$\hat{\phi}(\hat{t}) = \frac{1}{\{t_0 - (\hat{\gamma}_n/3)\hat{t}\}^3} \tag{48}$$

The parameter t_0 is given by the initial amplitude, $t_0 = \hat{\phi}(0)^{-1/3}$. The solution expresses an explosive growth. The typical time scale to approach the saturation level is $\tau_{Ap}\hat{\gamma}_n^{-1}\hat{\phi}(0)^{-1/3}$. Even if the initial amplitude is 10^{-3} times smaller compared to the saturation level, it takes only 10 times of $\tau_{Ap}\hat{\gamma}_n^{-1}$ to come to the strong turbulence level.

2.4.2 Approach to Saturation

We next study the approach to the stationary state. In the vicinity of the stationary condition, $\hat{\chi} = \hat{\chi}_{H0}$, Eq.(5) reduces to the formula of the strong turbulence

$$\mu \simeq \frac{T}{eB}\frac{e\tilde{\phi}}{T} \tag{49}$$

(T being the plasma temperature), and χ and λ are given through Eqs.(6) and (7) as $\chi = \frac{T}{eB}\frac{e\tilde{\phi}}{T}$ and $\lambda = \frac{T}{eB}\frac{e\tilde{\phi}}{T}\left(\frac{c}{a\omega_p}\right)^2$, respectively. The growth rate of the mode, Eq.(33), is then expressed as

$$\hat{\gamma} = \hat{\gamma}_s(1-\hat{\phi}) \tag{50-1}$$

and

$$\hat{\gamma}_s = \frac{0.45\sqrt{G_0}}{\left(1+\frac{0.02}{G_0}\omega_{E1}^2\right)} \tag{50-2}$$

The equation which descries the evolution of the fluctuation amplitude is given as

$$\frac{d}{d\hat{t}}\hat{\phi} = \hat{\gamma}_s(1-\hat{\phi})\hat{\phi} \tag{51}$$

This equation gives the solution

$$\hat{\phi}(\hat{t}) = \frac{\hat{\phi}(0)\exp(\hat{\gamma}_s\hat{t})}{1+\hat{\phi}(0)\{\exp(\hat{\gamma}_s\hat{t})-1\}} \tag{52}$$

The state $\hat{\phi} = 1$ is realized in the long time limit. The characteristic time scale, by which the stationary state is realized, is given by $\hat{\gamma}_s^{-1}\tau_{Ap}$.

The nonlinear behaviours of the self-sustained turbulence, i.e., those in the nonlinear growth phase and in the saturation phase, are summarized in the table 1.

The conventional argument in the quasi-linear picture is also compared in this table. In the zero-amplitude limit, where χ and μ are the second order in terms of the fluctuation amplitude $\tilde{\phi}$, Eq.(5) reduces to the formula of random walk, $\chi \simeq (k_\perp \tilde{\phi}/2B)^2 \gamma^{-1} = (\tilde{v}_{E\times B})^2 \gamma^{-1}$, where $\tilde{v}_{E\times B}$ is the fluctuating $E\times B$ velocity. If one substitutes the fluctuation level for the weak turbulence theory, $\tilde{v}_{E\times B} \simeq \gamma_{linear}/k_\perp$, χ is given as $\chi \simeq \gamma_{linear}/k_\perp^2$, which is the well known Kadomtsev formula [5].

3. Analysis in the Case of Magnetic Well

3.1 Model

We study a circular plasma with the toroidal coordinate (r, θ, ζ) and use the reduced set of equations with same variables (ϕ, J, p) [24]. In this section, the case where the magnetic curvature is no longer constant but has the poloidal dependence is considered. Instead of the interchange mode, the ballooning mode becomes the relevant mode for the analysis. The ballooning transformation [25] with the ballooning coordinate η is employed, and the eigenmode equation for the dressed test mode is given analogous to Eq.(1) as [11]

$$\frac{d}{d\eta}\frac{F}{\hat{\gamma}+\Lambda F^2}\frac{d}{d\eta}\left(\hat{\gamma}+KF+\hat{\omega}_{E1}\frac{d}{d\eta}\right)p+\alpha\{\kappa+\cos\eta+(s\eta-\alpha\sin\eta)\sin\eta\}\,p$$
$$-\left(\hat{\gamma}+MF+\hat{\omega}_{E1}\frac{d}{d\eta}\right)F\left(\hat{\gamma}+KF+\hat{\omega}_{E1}\frac{d}{d\eta}\right)p=0 \qquad (53)$$

where $K=\hat{\chi}n^2q^2$, $M=\hat{\mu}n^2q^2$, $\Lambda=\hat{\lambda}n^4q^4$, κ is the average curvature ($\kappa<0$ for the case of the magnetic well), α is the normalized pressure gradient, $\alpha=-q^2 R\, d\beta/dr$, s is the shear parameter $-rq'/q$, and F is redefined as $F=1+(s\eta-\alpha\sin\eta)^2$. The transport coefficient in the stationary state was also obtained by renormalizing the nonlinear interactions [3]. The parameter to indicate the inhomogeneity of the radial electric field, $\hat{\omega}_{E1}$, is defined as

$$\hat{\omega}_{E1} = \tau_{Ap} \frac{1}{s\hat{r}B} \frac{dE_r}{dr} \tag{54}$$

where $\hat{\omega}_{E1} = \omega_{E1} / s\hat{r}$ in comparison to Eq.(4).

3.2 Dynamics near Stationary State

The same method as in § 2 is applied to estimate the growth rate. We introduce the normalized mode number N

$$N = (\hat{\chi}\hat{\mu}/\alpha)^{1/4} nq \tag{55}$$

and the ratio H, instead of Eq.(14), as [3,11]

$$H = \frac{\alpha^{3/2}\hat{\lambda}}{\hat{\chi}^{3/2}\hat{\mu}^{1/2}} \tag{56}$$

As in the case of the interchange mode turbulence, the quantity H and the normalizing mode number $(\alpha/\hat{\chi}\hat{\mu})^{1/4}$ are treated as the dynamical variables.

The eigenmode equation Eq.(53) can be rewritten in a form similar to Eq.(8). The operators L_0, L_1, L_{t0} and L_{t1} are redefined as

$$L_0 = \frac{d^2}{d\eta^2} + \frac{\Lambda\alpha}{K}\{\kappa + \cos\eta + (s\eta - \sin\eta)\sin\eta\} - M\Lambda F^3 \tag{57}$$

$$L_1 = \frac{K}{F}\frac{d^3}{d\eta^3} - \frac{(M+K)}{K}\Lambda F^2 \frac{d}{d\eta} \tag{58}$$

$$L_{t0} = \left(\frac{1}{\Lambda F^2} - \frac{1}{KF}\right)\frac{d^2}{d\eta^2} + \frac{(K+M)}{K}\Lambda F^2 \tag{59}$$

$$L_{t1} = \frac{1}{K\Lambda F^3}\frac{d^3}{d\eta^3} + \frac{2\Lambda}{K} F \frac{d}{d\eta} \tag{60}$$

In deriving Eqs.(57) to (60), the operators d/dη and F are commuted, because the Weber type approximation for $(s-\alpha)^2\eta^2 << 1$ is used in the analytic study. (See [2] for the relevance of this approximation.)

The eigenmode for the unperturbed operator L_0 are given analytically by Weber functions in the small $\hat{s}$ limit, as in §2. In the steady state, the dynamical variables H and N take the eigenvalues as $H = H_0$ and $N^2 = N^{*2}$. The eigen values H_0 and N^{*2} were given as

$$H_0 = f(\hat{s}) \tag{61}$$

$$N^{*2} = 1/\sqrt{2 + C(\hat{s})} \tag{62}$$

with

$$\xi = \frac{(1-2\hat{s})(1+C(\hat{s}))}{(2+C(\hat{s}))} \tag{63}$$

where

$$f(s) = (1-2\hat{s})\sqrt{2+C(\hat{s})} \tag{64}$$

$\hat{s} = s - \alpha$, and $C(\hat{s}) = 6\hat{s}^2(1-2\hat{s})^{-1}$ [2].

The same procedure as in Eqs.(22) and (23) is applied for the case of the ballooning mode turbulence with Eqs. (57)-(60). Evaluating integrals (see appendix A for details) we have, similar to Eq.(26), as

$$<0|L_0|0> - \frac{<0|L_1|1><1|L_1|0>}{<1|L_0|1>}\hat{\omega}_{E1}^2 = \xi\left(\frac{\hat{\chi}_{L0}}{\hat{\chi}} - 1 - \bar{h}_1\,\hat{\omega}_{E1}^2\right) \tag{65}$$

$$\bar{h}_1 = \frac{1}{\alpha}\left\{\frac{F^2}{(1-2\hat{s})(1+C(\hat{s}))} + \frac{3\alpha F^{-1}}{4f(\hat{s})(2+C(\hat{s}))^{1/2}}\right\}^2 \tag{66}$$

In this expression, $\hat{\chi}_{L0}$ and $\bar{h}_1$ are those for tokamaks. The suffix 0 also indicates the statistical estimate value in the stationary state. Transport coefficients in the stationary H-mode and the stationary L-mode are given as

$$\hat{\chi}_{H0} = \frac{\hat{\chi}_{L0}}{1 + \bar{h}_1 \hat{\omega}_{E1}^2} \tag{67}$$

and

$$\hat{\chi}_{L0} = \frac{\alpha^{3/2}}{f(\hat{s})} \frac{\hat{\lambda}}{\hat{\chi}} \left(\frac{\hat{\chi}}{\hat{\mu}} \right)^{1/2} \tag{68}$$

respectively [11]. The formula $\hat{\chi}_{H0}$ is a general one for the transport coefficient in the stationary state, and $\hat{\chi}_{L0}$ is the specific expression in the limit of $\hat{\omega}_{E1} = 0$.

When the state is slightly deviated from the stationary solution and the dynamical variable $\hat{\chi}$ is different from $\hat{\chi}_{H0}$, the growth rate γ is calculated. Using the formula Eq.(22) and evaluation Eq.(65), $\hat{\gamma}$ is expressed as

$$\Gamma \hat{\gamma} = \xi \frac{\hat{\chi}_L}{\hat{\chi}} \left\{ 1 - \frac{\hat{\chi}}{\hat{\chi}_{H0}} \right\} \tag{69}$$

The multiplication factor Γ is evaluated by using integrals <ilLlj>, which are given in the appendix A, as

$$\Gamma = \frac{H}{\sqrt{\alpha}} (\Gamma_0 + \Gamma_E \hat{\omega}_{E1}^2) \tag{70}$$

where the coefficients Γ_0 and Γ_E are given as

$$\Gamma_0 \simeq \frac{2F^2}{2 + C(\hat{s})} + \frac{1 + C(\hat{s})}{2F(2 + C(\hat{s}))^{3/2}} \tag{71}$$

and

$$\Gamma_E \simeq \frac{1}{\alpha}\left\{\frac{f(\hat{s})F^4}{(2+C(\hat{s}))^{3/2}} + \left(\frac{F^2}{2+C(\hat{s})} - \frac{3F^4}{4(2+C(\hat{s}))^2} - \frac{F^7}{(1+C)(2+C(\hat{s}))^{3/2}}\right)\right\} \tag{72}$$

with $F \simeq 1 + \hat{s}^2/2\xi$. From these results, we have the growth rate near the stationary ballooning mode turbulence, similar to Eq.(33), as

$$\hat{\gamma} = \sqrt{\alpha}\,\frac{\xi}{(\Gamma_0 + \Gamma_E \hat{\omega}_{E1}^2)}\left\{1 - \frac{\hat{\chi}}{\hat{\chi}_H}\right\} \tag{73}$$

In the limit of $s = \alpha$, we obtain an analytic expression as

$$\hat{\gamma} = \frac{0.42\,\alpha^{1/2}}{1 + 0.39\alpha^{-1}\,\hat{\omega}_{E1}^2}\left(1 - \frac{\hat{\chi}}{\hat{\chi}_H}\right) \tag{74}$$

The growth/damping rate is expressed as the first order term with respect to $(\hat{\chi}/\hat{\chi}_{H0} - 1)$ near the stationary state.

3.3 Nonlinear Growth in Low Fluctuation Limit

3.3.1 Nonlinear Growth Rate

The argument on the growth rate for the limit of low fluctuation level (i.e., small χ limit) is also developed for the ballooning mode turbulence. The analytic formula in the strong shear limit was given as $\hat{\gamma} \simeq \hat{\lambda}^{1/5}(nq)^{4/5}\,\alpha^{3/5}\,s^{-2/5}$ [3]. It is extended to the case where the radial electric field shear is present, as

$$\hat{\gamma} = \frac{0.9\,\alpha^{3/5}\,\hat{\lambda}^{1/5}\,\hat{s}^{-2/5}(nq)^{4/5}}{1 + \frac{9}{20}\frac{\omega_{E1}^2\,\hat{s}^2}{\alpha\,s^2}} \tag{75}$$

The detailed derivation is given in Appendix B.

The characteristic mode number in the stationary state turbulence is given by the relation $N = N^*$ as is shown schematically in Fig.2. This relation gives the estimate of the toroidal mode number for the stationary state as $n^*q = N^*(\alpha/\hat{\mu}_{L0}\hat{\chi}_{L0})^{1/4}$. Using the eigen value N^* of Eq.(62), and the formula for $\hat{\chi}_{H0}$ of Eq.(68), the value of n*q is expressed in terms of the equilibrium parameters. Substituting this form of n* into the expression of γ, Eq.(75), the growth rate for this mode is estimated in the limit of small amplitude as

$$\hat{\gamma} = \frac{f(\hat{s})^{-1/5} s^{-2/5} \alpha^{1/2}}{1 + \left(\frac{9\hat{s}^2}{20\alpha s^2} - \frac{\bar{h}_1}{5}\right)\omega_{E1}^2} \left(\frac{\hat{\chi}}{\hat{\chi}_{H0}}\right)^{1/5} \tag{76}$$

Singular dependence as $(\chi/\chi_L)^{1/5}$ is also obtained for the small value of χ.

3.3.2 Connection Formula

Figure 4 compares the numerical solution of the eigenmode equation Eq.(53) with the analytic estimates Eq.(74) and Eq.(76). For fixed values of the mode number and other equilibrium parameters, the growth rate is calculated as a function of the thermal diffusivity χ. In the small χ limit, γ scales as $\chi^{1/5}$; in the large χ case, γ behaves like $(1 - \chi/\chi_s)$ (χ_s being the stability boundary). A simple interpolation

$$\hat{\gamma} \propto \left(\frac{\hat{\chi}}{\hat{\chi}_s}\right)^{1/5}\left(1 - \frac{\hat{\chi}}{\hat{\chi}_s}\right) \tag{77}$$

is found to be a good approximation for the fixed value of k_θ.

The mode with the higher toroidal mode number has the larger growth rate if $\hat{\chi}$ is much smaller than $\hat{\chi}_{H0}$. The largest growth rate at higher toroidal mode numbers remains of the order of $\alpha^{1/2}$ in the zero χ limit. (If the toroidal mode number is too high, the stabilization by the thermal diffusion and viscosity dominates.) Figure 5 illustrates the growth rate as a function of the anomalous transport coefficient. The ballooning mode turbulence has also the nature of the strong subcritical turbulence, so

that the rate of change in the presence of fluctuations completely differs from the result in the quasi-linear theory. The higher-n modes have larger growth rates in the case of the small values of $\hat{\chi}$. However, they are more easily stabilized when $\hat{\chi}$ is increased. One can consider the envelop of the peak of the growth rate. Equation (73) would serve as an approximate formula for the envelope of the largest growth rate.

3.4 Explosive Growth and Saturation

We see that the evolution equations for dynamical variables $\hat{\chi}$, $\hat{\mu}$, $\hat{\lambda}$, $\hat{\gamma}$ and $\tilde{\phi}$ has the same structure in the case of the ballooning mode turbulence as that for the interchange mode turbulence. The same argument in the section 2.4 applies.

The explosive growth of the mode is also derived from the formula of the growth rate in Eq.(76). The dynamical equation for the turbulence level has the same structure for the case of the interchange mode turbulence in the section 2. The explosive solution is obtained in the stage of the nonlinear growth as

$$\hat{\phi}(\hat{t}) = \frac{1}{\left\{\hat{\phi}(0)^{-1/3} - (\hat{\gamma}_n/3)\hat{t}\right\}^3} \tag{78}$$

For the case of the ballooning mode turbulence, the normalized value $\hat{\gamma}_n$ is claculated by use of Eqs.(67), (68) and (76). It is given as

$$\hat{\gamma}_n \approx \frac{1}{1 + \frac{3\hat{s}^2}{8\alpha s^2}\omega_{E1}^2} \frac{\alpha^{2/3}}{(sf(\hat{s}))^{1/3}} \left(\frac{c}{a\omega_p}\hat{k}_\perp\right)^{1/3} \tag{79}$$

The approach to the saturation state is also obtained near the stationary state. Introducing the normalized value $\hat{\gamma}_s$ as

$$\hat{\gamma}_s = \sqrt{\alpha}\,\frac{\xi}{(\Gamma_0 + \Gamma_E\hat{\omega}_{E1}^2)} \tag{80}$$

the evolution of the fluctuation amplitude is given, in the vicinity of the saturation state, as

$$\hat{\phi}(\hat{t}) = \frac{\hat{\phi}(0)\exp(\hat{\gamma}_s \hat{t})}{1 + \hat{\phi}(0)\{\exp(\hat{\gamma}_s \hat{t}) - 1\}} \tag{81}$$

The recovery of the stationary state is predicted.

4 Summary and Discussion

In this article, we have derived the formulae that describe the temporal change of turbulent fluctuations in toroidal plasmas. The rate of the dynamic change were investigated in the vicinity of the stationary state as well as in the nonlinear growing phase. Near the stationary state, the derivation from the self-sustained stationarily-turbulent state was analyzed by the perturbation method. Analytic formula of the nonlinear growth was obtained. The influences of the pressure gradient as well as the inhomogeneous electric field were quantified. The interchange mode turbulence was studied in the system of the magnetic hill, and the ballooning mode turbulence was investigated in the case of magnetic well, respectively.

The result is summarized in Table 2. The two cases (i.e., the interchange and ballooning modes) have a strong similarity to each other. The structure in Eq.(73) is the same as that of Eq.(33), although numerical coefficients are different. Quantities G_0 and α play the same role as the driving force, and ω_{E1} and $\hat{\omega}_{E1}$ play the role for suppression. In the cases of the magnetic hill and magnetic well, the dynamical equation for the fluctuation amplitude $\tilde{\phi}$ is generally given as

$$\frac{\partial}{\partial t}\tilde{\phi} = \gamma \tilde{\phi} \tag{82}$$

and

$$\gamma \approx \frac{(G_0 \text{ or } \alpha)^{1/2}}{1+h\omega_{E1}^2}\left(1-\frac{\chi}{\chi_{H0}}\right)\tau_{Ap}^{-1} \simeq \frac{(G_0 \text{ or } \alpha)^{1/2}}{1+h\omega_{E1}^2}\left(1-\frac{\tilde{\phi}}{\tilde{\phi}_{H0}}\right)\tau_{Ap}^{-1} \qquad (83)$$

This equation covers both the cases of the dynamics near the stationary state and the nonlinear growth in the small amplitude fluctuations. The connection formula is thus obtained. Equations (82) and (83) are the generic form of the dynamic structure in the self-sustained turbulence in toroidal plasmas.

The turbulent level changes in the fast time scale that is typical to the ideal MHD instabilities. This fast growth (when $\chi < \chi_H$) or damping (when $\chi > \chi_H$) occurs independent of the critical β value against the linear MHD instabilities. The growth rate is already considerably different from that of the linear mode calculations, even at the small-but-finite amplitude fluctuations. Our analysis shows that the plasma turbulence has the feature of the strong sub-critical turbulence.

The rapid rates, in the change of the turbulence level and the transport coefficient, provide the basis for the approximation which had been used in the study of H-mode dynamics and causality [17]. At the L/H transition and the ELM bursts, the electric field was predicted to change with the time scale of ν_i (ν_i being the ion-ion collision frequency). From Eq.(83), we see that the delay time in the change of fluctuations, which would follow the change of the radial electric field, is predicted to be of the order of $\tau_{Ap}\alpha^{-1/2}$. The delay of the turbulence change is negligible if the condition

$$\alpha > (\tau_{Ap}\nu_i)^2 \qquad (84)$$

is satisfied. The right hand side of Eq.(84) is much smaller than unity. This condition is usually satisfied for the plasma that is relevant to the H-mode. The simultaneous change in the transport coefficient, which was employed in [12,17], is now confirmed to be a relevant assumption. Some of the recent studies employed the dynamical equation for the fluctuations (See [18] and following work, or [26]). The nonlinear

theory in this article gives considerably different dependence of γ on the equilibrium parameters compared to these studies. The characteristics of the solution such as the bifurcation and the limit cycle solution, in general, can be changed by the choice of the form of the growth rate. For future quantitative study, it may be necessary to employ the formulae of Eqs.(33) and (73).

We here note that the fast change is predicted to take place even in the parameter region which is stable against the linear MHD mode. The linear ideal MHD theory has predicted that the fast growth rate of the order $\hat{\gamma} \simeq \sqrt{G_0}$ is possible to occur, if the pressure gradient exceeds the critical pressure gradient [27]

$$G_0 > G_{MHD} \simeq \frac{s^2}{4} \tag{85}$$

Our result indicate that, as a result of the nonlinear enhancement of the growth rate, the fast rate of change is possible even in the case of $G_0 < G_{MHD}$, if the turbulence level is deviated form that for the statistical expected value for the stationary state. In this sense, there is no threshold for the pressure gradient for this rapid change.

We finally note the relation with the transport catastrophe in the large pressure gradient limit [28]. In this article, the coefficient Γ is calculated analytically in the limit of a small pressure gradient. The first order correction of G_0 in Γ could be calculated. For simplicity, the result of the L-mode plasma with the interchange mode turbulence (i.e., in the absence of the radial electric field inhomogeneity) is presented. It is given as

$$\Gamma = \langle 0|L_{t0}|0\rangle \simeq \frac{H\left(2b + \frac{3}{2\xi}\right)}{G_0^{1/2}}\left[1 - \frac{3b}{(4/3)\xi^3 + 3H_0}\frac{G_0}{s^2}\right] \tag{86}$$

It should be noted that the sign of the second term in the square bracket is negative. If the pressure gradient is high enough to satisfy the condition, i.e.,

$$G_0 \geq \frac{(4/3)\xi^3 + 3H_0}{3b} s^2 \approx 5.6 s^2 \qquad (87)$$

the sign of the coefficient Γ becomes negative. If this is the case, the growth rate of the dressed-test mode becomes positive if χ exceeds the stationary solution χ_H. In other words, the stationary solution Eq.(35) is no longer thermodynamically stable. The catastrophe of the transport coefficient above a threshold pressure gradient may happen. This critical pressure is, however, much higher than the so called beta-limit against the ideal MHD stability, Eq.(85). The disappearance of the stable and stationary solution of Eq.(35) could happen if the pressure gradient becomes greater than the ideal MHD limit by an order of magnitude. The transport catastrophe was predicted to occur if the condition $G_0 > sr/R$ is satisfied [28]. The relation Eq.(87) indicate the new path for the transport catastrophe at the very steep pressure gradient. These processes would be important for the study of the beta limit phenomena in turbulent plasmas. This requires future study.

Acknowledgements

This article is dedicated to Prof. Kyoji Nishikawa on occasion of his sixtieth birthday. Authors wish to acknowledge continuous discussion with Dr. M. Azumi, and Dr. J. W. Connor. This work is partly supported by the Grant-in-Aid for Scientific Research of Ministry of Education, Culture and Science of Japan, by the collaboration programme of National Institute for Fusion Science, and by the collaboration programme of Advanced Fusion Center of Kyushu University.

Appendix A: Evaluation of Integral

The integrals are evaluated for the interchange mode turbulence. The Weber function approximation is used and integrals are given as

$$<0|L_{t0}|0> \simeq \frac{H}{\sqrt{G_0}}\sqrt{\frac{\mu}{\chi}}\left(\frac{\mu+\chi}{\mu}\frac{F^2}{b}+\frac{\xi}{2HF}-\frac{\xi}{2H^2}\frac{G_0}{s^2}\right) \tag{A1}$$

$$<1|L_{t0}|1> \simeq \frac{H}{\sqrt{G_0}}\sqrt{\frac{\mu}{\chi}}\left(\frac{\mu+\chi}{\mu}\frac{F^2}{b}+\frac{3\xi}{2HF}-\frac{3\xi}{2H^2}\frac{G_0}{s^2}\right) \tag{A2}$$

$$<1|L_{t1}|0> \simeq \frac{H}{G_0}\left(\sqrt{\frac{2}{b\xi}}-\sqrt{\frac{2\xi}{b}}F\right)+\frac{3\sqrt{2b}}{4}\frac{\chi}{\mu}\frac{Hs^2\xi^{3/2}}{F^3} \tag{A3}$$

$$<0|L_{t1}|1> \simeq \frac{H}{G_0}\left(\sqrt{\frac{2}{b\xi}}+\sqrt{\frac{2\xi}{b}}F\right)-\frac{3\sqrt{2b}}{4}\frac{\chi}{\mu}\frac{Hs^2\xi^{3/2}}{F^3} \tag{A4}$$

where F is approximated as an constant. Integrals $<i|L_{0,1}|j>$ were given in [25] as $<0|L_0|0> \simeq \xi(\chi_{L0}/\chi - 1)$, $<1|L_0|1> \simeq -2\xi$, $<0|L_1|1> \simeq -2bC_1G_0^{-1/2}$ and $<1|L_1|0> \simeq 2bC_2G_0^{-1/2}$ with $C_1 = 3\xi b/4 - 3/8 + H_0(b^2 + b/\xi + 3/4\xi^2)$ and $C_2 = C_1 - 1/2$. Taking the limit of $F \approx b$, we have the results Eqs.(30) and (31).

Integrals are also calculated in case of the ballooning mode turbulence. In the lowest order of α, the integrals in the small $\hat{s}$ limit is given as ($\hat{s} = s - \alpha$)

$$<0|L_{t0}|0> \simeq \sqrt{\frac{\chi}{\mu}}H\alpha^{-1/2}\left\{\frac{\mu+\chi}{\chi}N^4F^2+\frac{\xi}{2N^2FH}\left(1-\frac{\mu\alpha}{\chi N^2HF^2}\right)\right\} \tag{A5}$$

$$<1|L_{t0}|1> \simeq \sqrt{\frac{\chi}{\mu}}H\alpha^{-1/2}\left\{\frac{\mu+\chi}{\chi}N^4F^2+\frac{3\xi}{2N^2FH}\left(1-\frac{\mu\alpha}{\chi N^2HF^2}\right)\right\} \tag{A6}$$

$$<0|L_{t1}|1> \simeq \sqrt{2\xi}HN^2F\frac{1}{\alpha} \tag{A7}$$

$$<1|L_{t1}|0> \simeq -\sqrt{2\xi}HN^2F\frac{1}{\alpha} \tag{A8}$$

with $N = N^*(\hat{s})$. In performing the integral, the term F is also approximated as a constant $F \simeq 1 + \hat{s}^2/2\xi$. The expression of ξ is given in the text.

Integrals $<i|L_{0,1}|j>$ were given in [11] to give

$$<0|L_0|0> - \frac{<0|L_1|1><1|L_1|0>}{<1|L_0|1>}\hat{\omega}_{E1}^2 = \xi\left(\frac{\chi_{L0}}{\chi} - 1\right) - \xi\bar{h}_1\hat{\omega}_{E1}^2 \qquad (A9)$$

$$\bar{h}_1 = \frac{1}{\alpha}\frac{\chi}{\mu}\left\{\frac{\chi+\mu}{\chi}\frac{N^{*4}F^2}{2\xi} + \frac{3\alpha N^{*2}}{4H_0F}\right\}^2 \qquad (A10)$$

With the first order correction with respect to $\hat{\omega}_{E1}^2$, Γ is calculated as

$$\Gamma = \frac{H}{\sqrt{\alpha}}(\Gamma_0 + \Gamma_E\hat{\omega}_{E1}^2) \qquad (A11)$$

where Γ_0 and Γ_E are estimated as

$$\Gamma_0 \simeq \sqrt{\frac{\chi}{\mu}}\left\{\left(\frac{\chi+\mu}{\chi}\right)N^{*4}F^2 + \frac{\mu}{\chi}\frac{\xi}{2FH_0}\right\} \qquad (A12)$$

$$\Gamma_E \simeq \frac{1}{\alpha}\sqrt{\frac{\chi}{\mu}}\left\{\left(\frac{\chi+\mu}{2\chi}\right)H_0N^{*6}F^4 + \left(\frac{\chi+\mu}{2\chi}\right)^2\left(\frac{2\chi}{\chi+\mu}N^{*4}F^2 - \frac{3}{4}N^{*8}F^4 - \frac{\chi+\mu}{2\xi\mu}H_0N^{*12}F^7\right)\right\} \qquad (A13)$$

In calculating Γ_0 and Γ_E, the lowest order term with respect to α is kept.

If we employ the estimate that the Prandtl number is close to unity, $\mu/\chi \simeq 1$, and substitute the relations $N^* = (2 + C(\hat{s}))^{-1/4}$, $\xi = (1 - 2\hat{s})(1 + C(\hat{s}))(2 + C(\hat{s}))^{-1}$, and $H_0 = f(\hat{s})$, we have

$$\bar{h}_1 = \frac{1}{\alpha}\left\{\frac{F^2}{(1-2\hat{s})(1+C(\hat{s}))} + \frac{3\alpha F^{-1}}{4f(\hat{s})(2+C(\hat{s}))^{1/2}}\right\}^2 \qquad (A14)$$

$$\Gamma_0 \simeq \frac{2F^2}{2+C(\hat{s})} + \frac{1+C(\hat{s})}{2F(2+C(\hat{s}))^{3/2}} \qquad (A15)$$

$$\Gamma_E \simeq \frac{1}{\alpha}\left\{\frac{f(\hat{s})F^4}{(2+C(\hat{s}))^{3/2}} + \left(\frac{F^2}{2+C(\hat{s})} - \frac{3F^4}{4(2+C(\hat{s}))^2} - \frac{F^7}{(1+C)(2+C(\hat{s}))^{3/2}}\right)\right\} \tag{A16}$$

with $F \simeq 1 + \hat{s}^2/2\xi$. Substituting these integrals, Eq.(73) is obtained.

Appendix B: Growth Rate in the Limit of Small Transport Coefficients

B.1 Interchange Mode

Analytic formula of the growth rate in the limit of the low transport coefficient, $\hat{\chi} << \hat{\chi}_{H0}$, has been discussed. The dependence like $\hat{\gamma} \propto \hat{\lambda}^{1/5}$ has been derived [3]. The analytic expression of γ, however, was limited in the case where the radial electric field shear is absent. We here generalize the analysis in the presence of the radial electric field shear.

We first study the case of the interchange mode. The basic equation was given as [25]

$$\frac{d}{dk}\frac{1}{\hat{\lambda}k_{\perp}^4}\frac{d}{dk}\left(\hat{\gamma}+\omega_E\frac{d}{dk}\right)\tilde{p}+\frac{G_0}{s^2}\tilde{p}-\frac{1}{s^2k_{\theta}^2}\left(\hat{\gamma}+\omega_E\frac{d}{dk}\right)k_{\perp}^2\left(\hat{\gamma}+\omega_E\frac{d}{dk}\right)\tilde{p}=0 \quad \text{(B1)}$$

where $\omega_E = k_\theta \omega_{E1}$, $\omega_{E1} = \tau_{Ap}(dE_r/dr)B^{-1}$ and the electrostatic limit is taken in the Ohm's law for the transparency of the argument. (This approximation does not affect the dependence like $\hat{\gamma} \propto \hat{\lambda}^{1/5}$.) Keeping the first order correction with respect to ω_E, Eq.(B1) is written as

$$L_0\tilde{p}+\frac{\omega_{E1}}{\hat{\gamma}}L_1\tilde{p}=0 \quad \text{(B2)}$$

where

$$L_0=\frac{d}{dy}\frac{1}{1+y^2}\frac{d}{dy}+g-\Omega(1+y^2) \quad \text{(B3)}$$

$g = G_0\hat{\lambda}k_\theta^4 s^{-2}\hat{\gamma}^{-1}$, $\Omega = \hat{\gamma}\hat{\lambda}k_\theta^4 s^{-2}$ and

$$L_1=\frac{d}{dy}\frac{1}{1+y^2}\frac{d^2}{dy^2}-2\Omega\left(\frac{d}{dy}+\frac{y}{1+y^2}\right) \quad \text{(B4)}$$

(Note that Ω is the parameter which describes the growth rate in this appendix, and must be distinguished form the magnetic curvature Ω' in the main text.)

The eigen value equation is solved by use of the variational method. The functional is introduced as

$$\bar{R} = \int_{-\infty}^{\infty} p^* \, (L_0 + (\omega_{E1}/\hat{\gamma}) L_1) \, p \, dk \tag{B5}$$

where the asterisk * denotes the complex conjugate. We set the trial functions as

$$\tilde{p} = u_0 + (\rho_r + i \, \rho_i) u_1 \tag{B6}$$

where

$$u_0(y) \equiv \frac{\sigma^{1/2}}{\pi^{1/4}} \exp\left(-\frac{\sigma^2 y^2}{2}\right) \tag{B7-1}$$

$$u_1(y) \equiv \frac{2^{1/2}\sigma}{\pi^{1/4}} \, y \exp\left(-\frac{\sigma^2 y^2}{2}\right) \tag{B7-2}$$

(Note that σ is not conductivity in the appendix B.) The functional $\bar{R}$ is given

$$\begin{aligned} \bar{R} = & < u_0 | L_0 | u_0 > + (\rho_r^2 + \rho_i^2) < u_1 | L_0 | u_1 > \\ & + (\rho_r + i\rho_i) \frac{\omega_{E1}}{\hat{\gamma}} < u_0 | L_1 | u_1 > + (\rho_r - i\rho_i) \frac{\omega_{E1}}{\hat{\gamma}} < u_1 | L_1 | u_0 > \end{aligned} \tag{B8}$$

The eigenvalue equation is given as

$$\frac{\partial}{\partial \rho_r} \bar{R} = 0, \quad \frac{\partial}{\partial \rho_i} \bar{R} = 0, \quad \frac{\partial}{\partial \sigma} \bar{R} = 0 \quad \text{and} \quad \bar{R} = 0 \tag{B9}$$

Solving the parameter $\rho_r + i\rho_i$ from the relation $\partial \bar{R} / \partial \rho_{r,i} = 0$, and substituting it into Eq.(B8), we have

$$\bar{R} = < u_0|L_0|u_0 > - \left(\frac{\omega_{E1}}{\hat{\gamma}}\right)^2 \frac{< u_0|L_1|u_1 >< u_1|L_1|u_0 >}{< u_1|L_0|u_1 >} \qquad \text{(B10)}$$

where the lowest order correction with respect to ω_{E1} is kept. The integral is performed and we have

$$< u_0|L_0|u_0 > = -\sigma^4 + \frac{2}{\sqrt{\pi}}\sigma^5 \exp(\sigma^2)\mathrm{Erfc}(\sigma) + g - \Omega - \frac{\Omega}{2\sigma^2} \qquad \text{(B11)}$$

We find, *a posteriori,* an ordering $\sigma \propto \Omega^{1/6}$ and σ is a smallness parameter (so is Ω). We therefore keep the lowest order term with respect to σ. In the absence of the radial electric field inhomogeneity ($\omega_{E1} = 0$), we have

$$\bar{R} \simeq -\sigma^4 + g - \Omega - \frac{\Omega}{2\sigma^2} \qquad \text{(B12)}$$

Substituting this expression into Eq.(B9) and taking the optimum with respect to the variation of σ, we have

$$\sigma = 2^{-1/3}\,\Omega^{1/6} \qquad \text{(B13-1)}$$

and

$$g = \frac{3}{2^{4/3}}\,\Omega^{2/3} + \Omega \simeq \frac{3}{2^{4/3}}\,\Omega^{2/3} \qquad \text{(B13-2)}$$

or

$$\hat{\gamma} = \hat{\gamma}_0 \simeq 2^{4/5} 3^{-3/5} G_0^{3/5} \hat{\lambda}^{1/5} s^{-2/5} k_\theta^{4/5} \qquad \text{(B14)}$$

This recovers the previous theory for the current diffusive interchange mode.

Other integrals are calculated, in the lowest order of σ, as

$$< u_1|L_0|u_1 > = -2\sqrt{\pi}\sigma^3 + g - \Omega - \frac{3\Omega}{2\sigma^2} \simeq -2\sqrt{\pi}\sigma^3 \qquad \text{(B15-1)}$$

$$< u_0|L_1|u_1 > = -\frac{6}{\sqrt{2}}\sigma^5 - 3\sqrt{2}\Omega\sigma \simeq -\frac{6}{\sqrt{2}}\sigma^5 \qquad \text{(B15-2)}$$

$$< u_1|L_1|u_0 > = \sqrt{2\pi}\sigma^4 - \sqrt{2}\Omega\sigma \simeq \sqrt{2\pi}\sigma^4 \qquad \text{(B15-3)}$$

The functional $\bar{R}$ is calculated as

$$\bar{R} \approx -\sigma^4 + g - \frac{\Omega}{2\sigma^2} - 3\left(\frac{\omega_{E1}}{\hat{\gamma}}\right)^2\sigma^6 \qquad \text{(B16)}$$

The correction with respect to ω_{E1} is in a higher order in σ. This correction does not affect the solution $\sigma = 2^{-1/3}\,\Omega^{1/6}$. By the help of this solution for σ, Eq.(B16) provides the dispersion relation as

$$g = \frac{3}{2^{4/3}}\Omega^{2/3}\left\{1 + \frac{1}{2^{2/3}}\left(\frac{\bar{\omega}_{E1}}{\hat{\gamma}_0}\right)^2\Omega^{1/3}\right\} \qquad \text{(B17)}$$

The $\Omega^{1/3}$ term in the bracket is evaluated in terms of the unperturbed value as $\Omega^{1/3} = 3\hat{\gamma}_0^2 / 2^{4/3}G_0$. In the presence of the radial electric field inhomogeneity, the growth rate is given as

$$\hat{\gamma} = \frac{\hat{\gamma}_0}{\left(1 + \frac{3}{4}\frac{\omega_{E1}^2}{G_0}\right)^{3/5}} \approx \frac{\hat{\gamma}_0}{1 + \frac{9}{20}\frac{\omega_{E1}^2}{G_0}} \qquad \text{(B18)}$$

The Lorentz form of the radial electric field correction is obtained. The suppression factor is very close to that for the transport coefficient, Eq.(27).

We here notice that the odd-parity mode is an weaker instability, compared to the even-parity mode, in the small λ limit. The growth rate of the odd-parity mode, in the $\omega_{E1} = 0$ limit, is given by use of the functional $\bar{R} \equiv < u_1|L_0|u_1 >$. The integral is

given by Eq.(B14-1). By finding the optimum with respect to σ, we have the dispersion relation $g \approx 5(4\pi)^{1/5}2^{-1}\,\Omega^{3/5}$, or

$$\hat{\gamma} \approx 5^{-5/8}(8/\pi)^{1/8}G_0^{5/8}\,\hat{\lambda}^{1/4}\,s^{-1/2}\,k_\theta \tag{B19}$$

The power index of λ is now 1/4 and is higher than the case of the even-mode. This result shows that the odd-parity mode is an weaker instability than the even-parity mode. (We notice that γ in Eq.(B19) has the fractional power dependence on λ. Though the growth rate is smaller than the even-parity mode, the odd-parity mode also shows the explosive growth in time.)

B.2 Ballooning Mode

We next study the case of the ballooning mode instability. The eigenmode equation (53) is expressed in the limit of $\chi, \mu \to 0$ as

$$L_0\tilde{p} + \frac{\omega_{E1}}{\hat{\gamma}}L_1\,\tilde{p} = 0 \tag{B20}$$

where

$$L_0 = \frac{d}{d\eta}\frac{1}{F}\frac{d}{d\eta} + \frac{\alpha\hat{\lambda}(nq)^4}{\hat{\gamma}}\{\cos\eta + (s\eta - \alpha\sin\eta)\sin\eta\} - F\hat{\lambda}(nq)^4\hat{\gamma} \tag{B21}$$

$$L_1 = \frac{1}{s}\frac{d}{d\eta}\frac{1}{F}\frac{d^2}{dy^2} - \frac{\hat{\lambda}(nq)^4\hat{\gamma}}{s}\left(F\frac{d}{d\eta} + \frac{d}{d\eta}F\right) \tag{B22}$$

and $F = 1 + (s\eta - \alpha\sin\eta)^2$. We study as in [3] the strongly localized mode. Analytic treatment of possible by taking the strong shear limit. We use the ordering $\hat{s}\eta \approx 1$ ($\hat{s} = s - \alpha$). In this limit, the approximations are derived as $F \approx 1 + \hat{s}^2\eta^2$ and $\cos\eta + (s\eta - \alpha\sin\eta)\sin\eta \approx 1$. Equations (B21) and B(22) are simplified as

$$L_0 = \frac{d}{dy}\frac{1}{1+y^2}\frac{d}{dy} + \frac{\alpha\hat{\lambda}(nq)^4}{\hat{\gamma}\hat{s}^2} - \frac{\hat{\gamma}\hat{\lambda}(nq)^4}{\hat{s}^2}(1+y^2) \tag{B23}$$

and

$$L_1 = \frac{\hat{s}}{s}\left\{\frac{d}{d\eta}\frac{1}{1+y^2}\frac{d^2}{dy^2} - \frac{\hat{\lambda}(nq)^4\hat{\gamma}}{\hat{s}^2}\left((1+y^2)\frac{d}{d\eta} + \frac{d}{d\eta}(1+y^2)\right)\right\} \tag{B24}$$

by changing the variables as $y = \hat{s}\eta$.

Comparing Eqs.(B23) and B(24) to Eqs.(B3) and (B4), we see that the same procedures apply by properly replacing parameters. We have the growth rate in the strong shear limit, $\hat{s} >> 1$, as

$$\hat{\gamma} = \frac{\hat{\gamma}_0}{1 + \frac{9}{20}\frac{\omega_{E1}^2\hat{s}^2}{\alpha s^2}} \tag{B25}$$

and

$$\hat{\gamma}_0 = 2^{4/5}3^{-3/5}\alpha^{3/5}\hat{\lambda}^{1/5}\hat{s}^{-2/5}(nq)^{4/5} \tag{B26}$$

The growth rate is in proportion to $\lambda^{1/5}$ in the zero ω_{E1} limit, which reproduces the previous analysis [3]. The Lorentzian form for the suppression by the radial electric field is obtained as well.

References

[1] Itoh K, Itoh S-I, Fukuyama A 1992 *Phys. Rev. Lett.* **69** 1050.

[2] Itoh K, Yagi M, Itoh S-I, Fukuyama A, Azumi M 1993 *Plasma Phys. Cont. Fusion* **35** 543.

----- 1993 *J. Phys. Soc. Jpn.* **62** 4269.

Yagi M, Itoh K, Itoh S-I, Fukuyama A, Azumi M 1993 *Phys. Fluids B* **5** 3702.

[3] Itoh K, Itoh S-I, Fukuyama A, Yagi M, Azumi M 1994 *Plasma Phys. Cont. Fusion* **36** 279.

[4] Itoh K, Itoh S-I, Fukuyama A, Yagi M, Azumi M 1994 *Plasma Phys. Cont. Fusion* **36** 1501.

[5] Kadomtsev B B 1965 *Plasma Turbulence* (Academic Press, New York).

[6] Fukuyama A, Itoh K, Itoh S-I, Yagi M, Azumi M 1995 *"Transport Simulation on L-mode and Improved Confinement Associated with Current Profile Modification", Plasma Phys. Contr. Fusion* **37** in press.

[7] Fukuyama A, Itoh K, Itoh S-I, Yagi M, Azumi M 1994 *Plasma Phys. Contr. Fusion* **36** 1385.

Yagi M, Itoh K, Itoh S-I, Fukuyama A, Azumi M 1994 *J. Phys. Soc. Jpn.* **63** 10.

[8] Simonen T C et al 1988 *Phys. Rev. Lett.* **61** 1720.

[9] JET Team 1988 in *Plasma Physics and Controlled Nuclear Fusion Research 1988* (IAEA, Vienna 1989) Vol.1, 215.

[10] Murmann H, Zohm H, ASDEX- and NI Team 1990 in *Proc. 17th EPS Conf. on Controlled Fusion and Plasma Heating* (Amsterdam) Vol.14B, Part I, p54.

Hoang G T et al 1994 *Nucl. Fusion* **34** 75.

Soeldner F X et al. 1994 *Nucl. Fusion* **34** 985.

[11] Itoh S-I, Itoh K, Fukuyama A, Yagi M 1994 *Phys. Rev. Lett.* **72** 1200.

[12] Itoh S-I, Itoh K 1988 *Phys. Rev. Lett.* **60** 2276.

Shaing K C, Crume E Jr 1989 *Phys. Rev. Lett.* **63** 2369.

[13] Wagner F et al 1982 *Phys. Rev. Lett.* **49** 1408.

[14] Itoh S-I, Itoh K, Fukuyama A, Yagi M, Azumi M, Nishikawa K 1994 *Phys. Plasmas* **1** 1154.

[15] Connor J W 1993 *Plasma Phys. Contr. Fusion* **35** 757.

[16] Itoh S-I, Itoh K 1990 *J. Phys. Soc. Jpn.* **59** 3815.

[17] Itoh S-I, Itoh K, Fukuyama A, Miura Y, JFT-2M Group 1991 *Phys. Rev. Lett.* **67** 2485.

Itoh S-I, Itoh K, Fukuyama A 1993 *Nucl. Fusion* **29** 1445.

See also Zohm H 1994 *Phys. Rev. Lett.* **71** 222.

[18] Diamond P H, Liang Y M, Carreras B A, Terry P W 1994 *Phys. Rev. Lett.* **72** 2565.

[19] Biglari H, Diamond P H, Terry P W 1990 *Phys. Fluids* B **2** 1.

Shaing K C, Crume E C Jr., Houlberg W A 1990 *Phys. Fluids* B **2** 1492.

Hinton F L 1991 *Phys. Fluids* B **3** 696.

[20] Strauss H 1980 *Plasma Phys.* **22** 733.

Hazeltine R D 1983: *Phys. Fluids* **26** 3242.

[21] Itoh K, Itoh S-I, Fukuyama A, Sanuki H, Yagi M 1994 *Plasma Phys. Contr. Fusion* **36** 123.

[22] Greene J, Johnson J L 1961 *Phys. Fluids* **4** 875.

[23] Yagi M et al 1995: '*Numerical Simulation of the Nonlinear Instability by Electron Inertia*', submitted to Phys. Rev. Lett.

[24] Strauss H 1977 *Phys. Fluids* **20** 1354.

[25] Connor J W, Hastie R J, Taylor J B 1979 *Proc. R. Soc.* A **365** 1.

[26] Stringer T E 1993 *Nucl. Fusion* **33** 1249.

Hassam A B, Drake J F 1993 *Phys. Fluids* B **5** 4022.

Sugama H et al. 1995 *Plasma Phys. Contr. Fusion* **37** 345.

[27] Shafranov V D, Yurchenko E I 1967 *Zh. Eksp. Teor. Fiz* **53** 1157 [*Sov. Phys. JETP* **26** 682].

[28] Itoh K et al 1995 '*Self-Sustained Magnetic Braiding in Toroidal Plasmas*', *Plasma Phys. Contr. Fusion* **37** in press.

Figure Captions

Fig. 1 Schematic drawing of the growth rate as a function of the turbulent transport coefficient (a). In the case of small but finite transport coefficient, the mode growth rate shows the strong nonlinear growth. This region is called as the nonlinear growing regime. When the transport level becomes high enough, the growth rate vanishes. This state is called as the stationary state. If the turbulent level vanishes, the growth rate of the linear theory, γ_{lin}, is recovered. The linearly-unstable case is shown by the solid line, and the dotted line indicates the linearly-stable case.

The stability boundary is shown in the plane of the equilibrium pressure gradient and the fluctuation level (b). The boundary I is the thermodynamically-stable, stationary turbulent level. The boundary II is the neutral line for the subcritical turbulence. The criterion $|\nabla p_c|$ indicates the linear stability boundary.

Fig.2 The stability boundary in the mode-number/transport coefficient plane. The least stable mode, $k_\theta = k^*$, determines the level of turbulence and transport coefficient at the stationary state. The thick dotted-dashed line indicates the peak of the growth rate. If the transport coefficient is smaller than the stationary value, the peak of the growth rate is realized by the mode with the higher mode numbers.

Fig.3 Growth rate of the dressed-test mode as a function of the transport coefficient (fluctuation level). The case of interchange turbulence is shown. The solid curve shows the case of $k_\theta = k^*$, Eq.(40). The coefficient C_I is given as $C_I = 0.45\left(1 + 0.02G_0^{-1}\omega_{E1}^2\right)^{-1}$Thin dotted curve shows the case of the shorter wave length $k_\theta > k^*$. Thick dashed line indicates Eq.(33) which is the envelope of the growth rate for various components. (In the case of the zero amplitude,

$\chi \to 0$, the growth rate should reduce to the from in the linear theory, γ_{linear}, but this limit is suppressed in this schematic graph.)

Fig. 4 The numerical solution of the eigenmode equation (53) is shown by the solid line. Parameters are: $\omega_{E1} = 0$, $\alpha = 0.432$, $n = 30$, $q = 3$, $\kappa = -0.111$, $s = 0.4$, $\lambda/\chi = 10^{-3}$, $\mu/\chi = 1$. For this case, the stability boundary χ_s is given as $\hat{\chi}_s = 5.2 \times 10^{-4}$. In the small χ limit, γ scales as $\chi^{1/5}$; in the large χ case, γ behaves like $(1 - \chi/\chi_s)$. A simple interpolation of the form $\hat{\chi}^{1/5}(1 - \hat{\chi}/\hat{\chi}_s)$ is shown by the dotted line.

Fig.5 Growth rate of the dressed-test mode for the case of the ballooning mode turbulence. The case of $k_\theta = k^*$, the interpolation of Eqs.(73) and (75), is shown by the solid curve. The coefficient C_B is given as $C_B = \xi(\Gamma_0 + \Gamma_E \omega_{E1}^2)^{-1}$. Thin dotted curve shows the case of the shorter wave length $k_\theta > k^*$. Thick dashed line indicates Eq.(73) which is the envelope of the growth rate for various components.

Table 1 Summary of Dynamics Relations

	Linear Mode	Self-Sustained Turbulence	
Range	$\chi \to 0$	$0 < \chi << \chi_{H0}$	$\chi \sim \chi_{H0}$
Growth Rate	γ_{linear}	$\gamma \propto (\chi/\chi_{H0})^{1/5}$	$\gamma \propto (1 - \chi/\chi_{H0})$
$\chi[\tilde{\phi}]$	$\propto \tilde{\phi}^2$	$\chi(\chi + \gamma k_\perp^{-2}) \sim (\tilde{\phi}/B)^2$	
		$\propto \tilde{\phi}^{5/3}$	$\propto \tilde{\phi}^1$
$\gamma[\phi]$	$\propto \phi^0$	$\propto \hat{\phi}^{1/3}$	$\propto (1 - \hat{\phi})$
$\phi(t)$	Exponential $\hat{\phi} \sim \exp(\gamma_{linear} t)$	Explosive $\hat{\phi} \sim (\hat{t}_0 - \hat{\gamma}_n \hat{t})^{-3}$	Saturating $\hat{\phi} \sim (1 + \exp(-\hat{t}))^{-1}$
χ_{theory}	$\gamma_{linear} k_\perp^{-2}$	-	χ_{H0}

Table 2 Summary of the Transport Coefficient and Dynamic Equation

Systems	**Magnetic Hill** (Torsatron/Heliotron, RFP)	**Magnetic Well** (Tokamak, Stellarator)
Driving Force	$G_0 = \Omega' \beta' / 2\varepsilon^2$	$\alpha = -Rq^2\beta'$
Relevant Mode	Interchange	Ballooning
Basic Equation	Eq.(1)	Eq.(53)
L-mode Transport ($\hat{\mu}_{L0} \simeq \hat{\mu}_{e,L0} \simeq \hat{\chi}_{L0}$)	$\hat{\chi}_{L0} \equiv \frac{G_0^{3/2}}{H_0 s^2} \frac{\hat{\lambda}}{\hat{\chi}} \left(\frac{\hat{\chi}}{\hat{\mu}}\right)^{1/2}$ (Eq.(29))	$\hat{\chi}_{L0} = \frac{\alpha^{3/2}}{f(\hat{s})} \frac{\hat{\lambda}}{\hat{\chi}} \left(\frac{\hat{\chi}}{\hat{\mu}}\right)^{1/2}$ (Eq.(67))
H-mode Transport ($\hat{\mu}_{H0} \simeq \hat{\mu}_{e,H0} \simeq \hat{\chi}_{H0}$)	$\hat{\chi}_{H0} \equiv \frac{\hat{\chi}_{L0}}{\left(1 + 0.52 G_0^{-1} \omega_{E1}^2\right)}$ ($\omega_{E1} = \tau_{Ap} E_r' / B$)	$\hat{\chi}_{H0} = \frac{\hat{\chi}_{L0}}{1 + \bar{h}_1 \hat{\omega}_{E1}^2}$ ($\bar{h}_1 \simeq 0.39/\alpha$, $\hat{\omega}_{E1} = \tau_{Ap} E_r' / \hat{r} s B$)
Typical Mode Number	$k_* \approx 0.6 \left(\frac{\chi}{\mu_e}\right)^{1/2} \frac{\omega_p}{c} G_0^{-1/2}$	$k_* \approx N^* f(\hat{s})^{1/2} \left(\frac{\chi}{\mu_e}\right)^{1/2} \frac{\omega_p}{c} \alpha^{-1/2}$
Fluctuation Level (Saturation Level)	$\frac{e\tilde{\phi}}{T} \simeq \chi_{H0} \frac{eB}{T}$	$\frac{e\tilde{\phi}}{T} \simeq \chi_{H0} \frac{eB}{T}$
Nonlinear Growth Rate (Near Stationary State)	$\hat{\gamma} = \frac{0.45 \sqrt{G_0}}{\left(1 + \frac{0.02}{G_0} \omega_{E1}^2\right)} \left(1 - \frac{\hat{\chi}}{\hat{\chi}_{H0}}\right)$	$\hat{\gamma} = \sqrt{\alpha} \frac{\xi}{\left(\Gamma_0 + \Gamma_E \hat{\omega}_{E1}^2\right)} \left(1 - \frac{\hat{\chi}}{\hat{\chi}_{H0}}\right)$
(Small Amplitude Limit)	$\hat{\gamma} = \frac{0.58 G_0^{1/2}}{1 + 0.35 \frac{\omega_{E1}^2}{G_0}} \left(\frac{\hat{\chi}}{\hat{\chi}_{H0}}\right)^{1/5}$	$\hat{\gamma} = \frac{f(\hat{s})^{-1/5} s^{-2/5} \alpha^{1/2}}{1 + \left(\frac{9\hat{s}^2}{20\alpha s^2} - \frac{\bar{h}_1}{5}\right) \omega_{E1}^2} \left(\frac{\hat{\chi}}{\hat{\chi}_{H0}}\right)^{1/5}$

Fig. 1

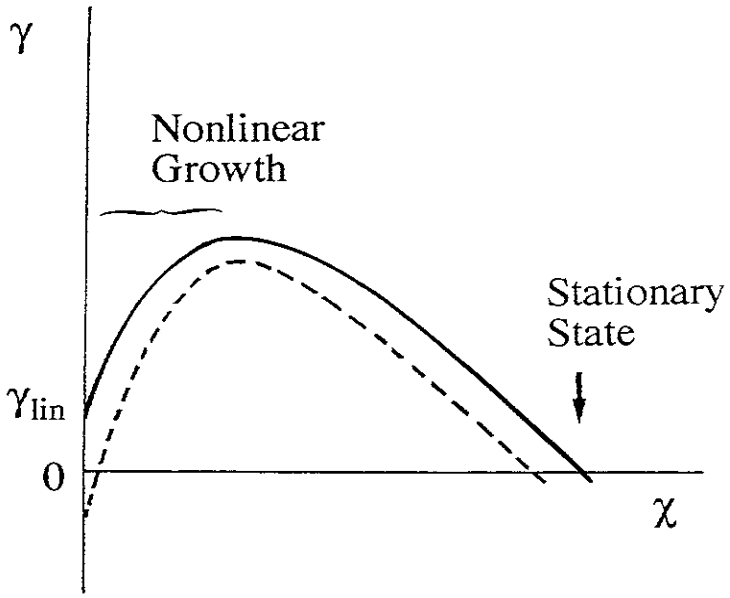
γ
(a)
Nonlinear
Growth
Stationary
State
γlin
0
χ

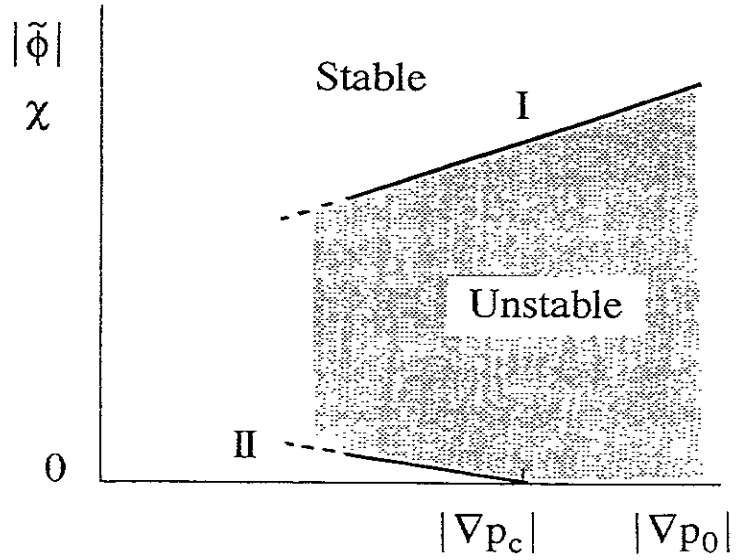
|φ̃|
χ
(b)
Stable
I
Unstable
II
0
|∇pc|
|∇p0|

Fig.2

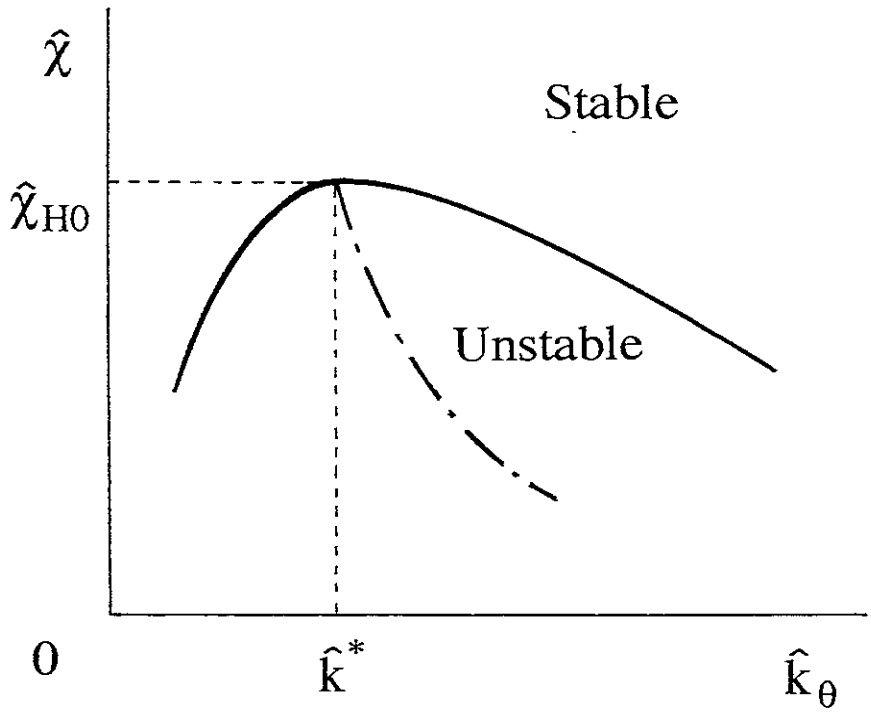

Fig.3

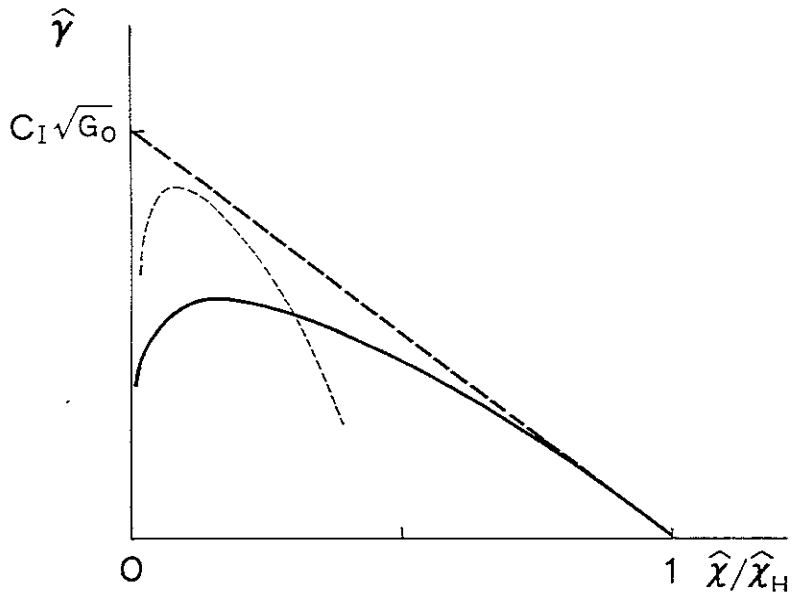

Fig. 4

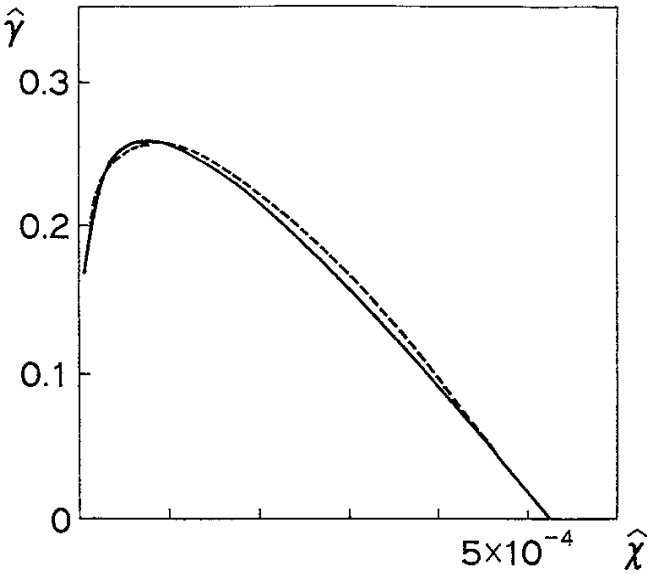

Fig.5

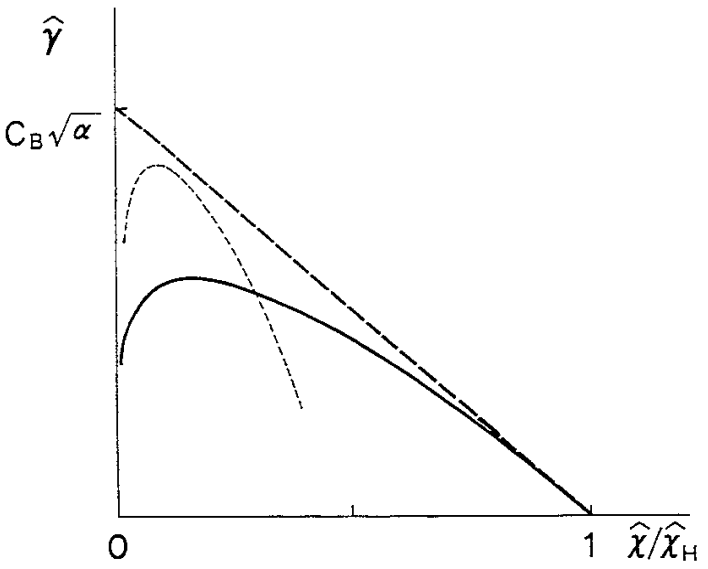

Recent Issues of NIFS Series

NIFS-311 K. Watanabe, T. Sato and Y. Nakayama,
Current-profile Flattening and Hot Core Shift due to the Nonlinear Development of Resistive Kink Mode; Oct. 1994

NIFS-312 M. Salimullah, B. Dasgupta, K. Watanabe and T. Sato,
Modification and Damping of Alfvén Waves in a Magnetized Dusty Plasma; Oct. 1994

NIFS-313 K. Ida, Y. Miura, S -I. Itoh, J.V. Hofmann, A. Fukuyama, S. Hidekuma, H. Sanuki, H. Idei, H. Yamada, H. Iguchi, K. Itoh,
Physical Mechanism Determining the Radial Electric Field and its Radial Structure in a Toroidal Plasma; Oct. 1994

NIFS-314 Shao-ping Zhu, R. Horiuchi, T. Sato and The Complexity Simulation Group,
Non-Taylor Magnetohydrodynamic Self-Organization; Oct. 1994

NIFS-315 M. Tanaka,
Collisionless Magnetic Reconnection Associated with Coalescence of Flux Bundles; Nov. 1994

NIFS-316 M. Tanaka,
Macro-EM Particle Simulation Method and A Study of Collisionless Magnetic Reconnection; Nov. 1994

NIFS-317 A. Fujisawa, H. Iguchi, M. Sasao and Y. Hamada,
Second Order Focusing Property of 210° Cylindrical Energy Analyzer; Nov. 1994

NIFS-318 T. Sato and Complexity Simulation Group,
Complexity in Plasma - A Grand View of Self- Organization; Nov. 1994

NIFS-319 Y. Todo, T. Sato, K. Watanabe, T.H. Watanabe and R. Horiuchi,
MHD-Vlasov Simulation of the Toroidal Alfvén Eigenmode; Nov. 1994

NIFS-320 A. Kageyama, T. Sato and The Complexity Simulation Group,
Computer Simulation of a Magnetohydrodynamic Dynamo II: Nov. 1994

NIFS-321 A. Bhattacharjee, T. Hayashi, C.C.Hegna, N. Nakajima and T. Sato,
Theory of Pressure-induced Islands and Self-healing in Three-dimensional Toroidal Magnetohydrodynamic Equilibria; Nov. 1994

NIFS-322 A. Iiyoshi, K. Yamazaki and the LHD Group,
Recent Studies of the Large Helical Device; Nov. 1994

NIFS-323 A. Iiyoshi and K. Yamazaki,
The Next Large Helical Devices; Nov. 1994

NIFS-324 V.D. Pustovitov
Quasisymmetry Equations for Conventional Stellarators; Nov. 1994

NIFS-325 A. Taniike, M. Sasao, Y. Hamada, J. Fujita, M. Wada,
The Energy Broadening Resulting from Electron Stripping Process of a Low Energy Au^- Beam; Dec. 1994

NIFS-326 I. Viniar and S. Sudo,
New Pellet Production and Acceleration Technologies for High Speed Pellet Injection System "HIPEL" in Large Helical Device; Dec. 1994

NIFS-327 Y. Hamada, A. Nishizawa, Y. Kawasumi, K. Kawahata, K. Itoh, A. Ejiri, K. Toi, K. Narihara, K. Sato, T. Seki, H. Iguchi, A. Fujisawa, K. Adachi, S. Hidekuma, S. Hirokura, K. Ida, M. Kojima, J. Koong, R. Kumazawa, H. Kuramoto, R. Liang, T. Minami, H. Sakakita, M. Sasao, K.N. Sato, T. Tsuzuki, J. Xu, I. Yamada, T. Watari,
Fast Potential Change in Sawteeth in JIPP T-IIU Tokamak Plasmas; Dec. 1994

NIFS-328 V.D. Pustovitov,
Effect of Satellite Helical Harmonics on the Stellarator Configuration; Dec. 1994

NIFS-329 K. Itoh, S-I. Itoh and A. Fukuyama,
A Model of Sawtooth Based on the Transport Catastrophe; Dec. 1994

NIFS-330 K. Nagasaki, A. Ejiri,
Launching Conditions for Electron Cyclotron Heating in a Sheared Magnetic Field; Jan. 1995

NIFS-331 T.H. Watanabe, Y. Todo, R. Horiuchi, K. Watanabe, T. Sato,
An Advanced Electrostatic Particle Simulation Algorithm for Implicit Time Integration; Jan. 1995

NIFS-332 N. Bekki and T. Karakisawa,
Bifurcations from Periodic Solution in a Simplified Model of Two-dimensional Magnetoconvection; Jan. 1995

NIFS-333 K. Itoh, S.-I. Itoh, M. Yagi, A. Fukuyama,
Theory of Anomalous Transport in Reverse Field Pinch; Jan. 1995

NIFS-334 K. Nagasaki, A. Isayama and A. Ejiri
Application of Grating Polarizer to 106.4GHz ECH System on Heliotron-E; Jan. 1995

NIFS-335 H. Takamaru, T. Sato, R. Horiuchi, K. Watanabe and Complexity Simulation Group,
A Self-Consistent Open Boundary Model for Particle Simulation in Plasmas; Feb. 1995

NIFS-336 B.B. Kadomtsev,
Quantum Telegragh : is it possible?; Feb. 1995

NIFS-337 B.B.Kadomtsev,
Ball Lightning as Self-Organization Phenomenon; Feb. 1995

NIFS-338 Y. Takeiri, A. Ando, O. Kaneko, Y. Oka, K. Tsumori, R. Akiyama, E. Asano, T. Kawamoto, M. Tanaka and T. Kuroda,
High-Energy Acceleration of an Intense Negative Ion Beam; Feb. 1995

NIFS-339 K. Toi, T. Morisaki, S. Sakakibara, S. Ohdachi, T.Minami, S. Morita, H. Yamada, K. Tanaka, K. Ida, S. Okamura, A. Ejiri, H. Iguchi, K. Nishimura, K. Matsuoka, A. Ando, J. Xu, I. Yamada, K. Narihara, R. Akiyama, H. Idei, S. Kubo, T. Ozaki, C. Takahashi, K. Tsumori,
H-Mode Study in CHS; Feb. 1995

NIFS-340 T. Okada and H. Tazawa,
Filamentation Instability in a Light Ion Beam-plasma System with External Magnetic Field; Feb. 1995

NIFS-341 T. Watanbe, G. Gnudi,
A New Algorithm for Differential-Algebraic Equations Based on HIDM; Feb. 13, 1995

NIFS-342 Y. Nejoh,
New Stationary Solutions of the Nonlinear Drift Wave Equation; Feb. 1995

NIFS-343 A. Ejiri, S. Sakakibara and K. Kawahata,
Signal Based Mixing Analysis for the Magnetohydrodynamic Mode Reconstruction from Homodyne Microwave Reflectometry; Mar.. 1995

NIFS-344 B.B.Kadomtsev, K. Itoh, S.-I. Itoh
Fast Change in Core Transport after L-H Transition; Mar. 1995

NIFS-345 W.X. Wang, M. Okamoto, N. Nakajima and S. Murakami,
An Accurate Nonlinear Monte Carlo Collision Operator; Mar. 1995

NIFS-346 S. Sasaki, S. Takamura, S. Masuzaki, S. Watanabe, T. Kato, K. Kadota,
Helium I Line Intensity Ratios in a Plasma for the Diagnostics of Fusion Edge Plasmas; Mar. 1995

NIFS-347 M. Osakabe,
Measurement of Neutron Energy on D-T Fusion Plasma Experiments; Apr. 1995

NIFS-348 M. Sita Janaki, M.R. Gupta and Brahmananda Dasgupta,
Adiabatic Electron Acceleration in a Cnoidal Wave; Apr. 1995

NIFS-349 J. Xu, K. Ida and J. Fujita,
A Note for Pitch Angle Measurement of Magnetic Field in a Toroidal Plasma Using Motional Stark Effect; Apr. 1995

NIFS-350 J. Uramoto,
Characteristics for Metal Plate Penetration of a Low Energy Negative Muonlike or Pionlike Particle Beam: Apr. 1995

NIFS-351 J. Uramoto,
An Estimation of Life Time for A Low Energy Negative Pionlike Particle Beam: Apr. 1995

NIFS-352 A. Taniike,
Energy Loss Mechanism of a Gold Ion Beam on a Tandem Acceleration System: May 1995

NIFS-353 A. Nishizawa, Y. Hamada, Y. Kawasumi and H. Iguchi,
Increase of Lifetime of Thallium Zeolite Ion Source for Single-Ended Accelerator: May 1995

NIFS-354 S. Murakami, N. Nakajima, S. Okamura and M. Okamoto,
Orbital Aspects of Reachable β Value in NBI Heated Heliotron/Torsatrons; May 1995

NIFS-355 H. Sugama and W. Horton,
Neoclassical and Anomalous Transport in Axisymmetric Toroidal Plasmas with Electrostatic Turbulence; May 1995

NIFS-356 N. Ohyabu
A New Boundary Control Scheme for Simultaneous Achievement of H-mode and Radiative Cooling (SHC Boundary); May 1995

NIFS-357 Y. Hamada, K.N. Sato, H. Sakakita, A. Nishizawa, Y. Kawasumi, R. Liang, K. Kawahata, A. Ejiri, K. Toi, K. Narihara, K. Sato, T. Seki, H. Iguchi, A. Fujisawa, K. Adachi, S. Hidekuma, S. Hirokura, K. Ida, M. Kojima, J. Koong, R. Kumazawa, H. Kuramoto, T. Minami,. M. Sasao, T. Tsuzuki, J.Xu, I. Yamada, and T. Watari,
Large Potential Change Induced by Pellet Injection in JIPP T-IIU Tokamak Plasmas; May 1995

NIFS-358 M. Ida and T. Yabe,
Implicit CIP (Cubic-Interpolated Propagation) Method in One Dimension; May 1995

NIFS-359 A. Kageyama, T. Sato and The Complexity Simulation Group,
Computer Has Solved A Historical Puzzle: Generation of Earth's Dipole Field; June 1995